9-18-2013 12:00 AM

Co-pyrolysis of Birchwood Bio-oil and Reduced Crude in a Mechanically Fluidized Reactor

Ryan Lance
The University of Western Ontario

Supervisor
Dr. Franco Berruti
The University of Western Ontario Joint Supervisor
Dr. Cedric Briens
The University of Western Ontario

Graduate Program in Chemical and Biochemical Engineering
A thesis submitted in partial fulfillment of the requirements for the degree in Master of Engineering Science

CO-PYROLYSIS OF BIRCHWOOD BIO-OIL AND REDUCED CRUDE IN A MECHANICALLY FLUIDIZED REACTOR

(Thesis format: Monograph)

by

Ryan Lance

Graduate Program in Chemical and Biochemical Engineering

A thesis submitted in partial fulfillment
of the requirements for the degree of
Master of Engineering Science

The School of Graduate and Postdoctoral Studies
The University of Western Ontario
London, Ontario, Canada

Abstract

Atmospheric Reduced crude (ARC) was co-pyrolyzed with 23-44 dry wt. % birchwood bio-oil at 480-530°C in a mechanically fluidized reactor (MFR) to investigate the feasibility of integrating bio-oil with heavy petroleum feedstocks into a Fluid Coker™. The liquid products of the bio-oil and ARC were predominately segregated into two separate phases. The product yields of valuable petroleum liquid products were significantly reduced during co-pyrolysis when compared to the pyrolysis of ARC.

The effects of removing the aqueous phase of bio-oil before co-pyrolysis were investigated by separating the aqueous phase from birchwood bio-oil utilizing a novel co-distillation technique with ARC. The resulting 19-29 wt. % bio-oil distillation residues were pyrolyzed in a MFR at 480-500°C. The pyrolyzed distillation residues resulted in higher valuable liquid yields with significantly lower water contents when compared to the co-pyrolysis bio-oil and ARC. Valuable liquid yields were lower when compared to the pyrolysis of ARC.

Keywords:

Coking, Pyrolysis, Bio-oil Upgrading, Co-processing, Co-pyrolysis, Petroleum Refinery Integration

Acknowledgements

Dr. Franco Berruti and Dr. Cedric Briens for creating ICFAR, obtaining funding for ICFAR and graduate students, information imparted in classes, and for guidance and input.

Alfredo Martinez for designing the stuffing box seal for the small MFR. This thesis would not have been possible without a reactor that could handle the pressure drop through a tar coated filter.

Rob Taylor for mechanical troubleshooting, mechanical design input, machine shop training, and drilling things correctly.

Caitlin Marshall for performing analytical analysis on liquid and solid products, analytical chemistry ideas, GCMS-FID sorting, and providing entertainment value.

Dr. Anil Jhawar for performing the experimental work on the model compound study, editing chapters 1-2 of this thesis, and providing advice in areas.

Dr. Ran Xu and Dr. Lorenzo Ferrante for ICFAR, engineering, mechanical, electrical, and analytical lab training.

Table of Contents

List of Tables

List of Equations

List of Figures

List of Abbreviations

Abbreviation	Meaning	Page
ARC	Atmospheric Reduced Crude	16
ASTM	American Society for Testing and Materials	
CDU	Crude Distillation Unit	15
CFB	Circulating Fluidized Bed	6
C/O	Catalyst to Oil	18
ESP	Electrostatic Precipitator	23
FCC	Fluid Catalytic Cracking	16
GC	Gas Chromatography	
HGO	Heavy Gas Oil	16
HHV	High Heating Values	35
ISO	International Organization for Standardization	
KF	Karl Fischer	
LCO	Light Cycle Oil	17
LHV	Lower Heating Value	
LGO	Light Gas Oil	16
LPG	Liquefied Petroleum Gas	16
MFR	Mechanically Fluidized Reactor	23
TCD	Thermal Conductivity Detector	36
VDU	Vacuum Distillation Unit	15
VGO	Vacuum Gas Oil	17
VRC	Vacuum Reduced Crude	17
wt. %	Percentage by Weight	
Δ	Difference	

Chapter 1: Introduction and Literature Review

Crude oils are currently used to meet approximately 31.5 % of the world's energy supply [1], and supply approximately 80% of the feedstocks used in chemical industries [2]. The economic development of newly industrializing countries, especially large countries such as China and India has greatly increased the demand for energy and petroleum products in recent decades, which will continue into the future.

Petroleum deposits are finite resources that are currently being consumed at a faster rate than the rate than new deposits are discovered. With increasing demand and low prospects of discovering new large conventional crude deposits, the petroleum industry has been adapting by integrating new feedstocks into their refineries. The current trend in the petroleum industry is to retrofit existing infrastructure and install new units to process crudes that are heavier and/or more acidic, natural bitumen (tar sands), and oil shale deposits that have been previously considered unprofitable, but now feasible due to the increased costs of conventional crudes [3]. The investment into unconventional crude infrastructure is potentially risky in some countries. Future carbon taxes could make unconventional crude production and processing processes economically unfeasible, depending on the severity of the taxes [4]. It would be sensible to focus the development of unconventional crude technologies in countries that have policies favorable to the production of unconventional crude, while focusing on the development of petroleum alternative technologies in countries that favor development of alternatives to petroleum.

It has been argued that biomass derived fuels are carbon neutral as the same amount of carbon dioxide released during the combustion of biomass is integrated into the plant from the atmosphere during photosynthesis [5]. Many governments give biofuel producers/consumers subsidies and fuel/carbon tax exemptions regardless of their estimated life cycle green house gas emissions [6-7]. Promoters of these government subsidies and tax exemptions consider these policies to be necessary to promote the production of unprofitable biofuels that would not compete in a free market [8].

1.1 Biomass

Biomass is biological material derived from living organisms or organisms that had died in recent times. The recent times component of the definition is used to differentiate biomass from fossil fuels, which formed over millions of years. Unlike petroleum and coal, biomass sources are renewable resources that have the potential to be formed at the same rate that they are being consumed [9].

While biomass sources include plant and animal material, the available quantity of low value animal derived biomass sources is much lower than the quantity of available low value plant biomass sources. Woolf et al. [10] made estimates of the global availability of sustainable biomass for pyrolysis. They estimated that the available quantity of animal manure for pyrolysis was only 8.3-9.9 wt. % of the available carbon for pyrolysis. As there is significantly more available plant biomass for pyrolysis, efforts to produce chemicals and fuels from biomass are primarily focused on plant biomass.

While it is possible to grow crops specifically for the purpose of producing chemicals and fuels, the resources, land, and labour used to grow and harvest energy crops could be productively used elsewhere. It is more desirable and economically justifiable to produce chemicals and fuels from low value feedstocks that currently aren't being used productively. Potential low value biomass feedstocks include forestry residues, agricultural residues, wood based industrial waste products, waste paper, and food waste.

The main components of plant biomass are cellulose, hemicellulose, and lignin. Cellulose is a linear polymer of β 1-4 linked D-glucose monomers. The monomers of hemicellulose vary depending on the biomass source, but hemicellulose monomers are usually composed of predominately pentose sugars with some glucose molecules. Lignin is a very complicated polymer that mostly consists of phenols and alcohols [11]. Lignin is the only known biomass source of aromatic compounds [12]. The chemical compositions of some samples of wood are listed in table 1.1.

Table 1.1 Chemical Compositions of Selected Wood Samples [13]

Composition (wt. %)	Scots Pine (*Pinus Sylvetris*)	Spruce (*Picea Glauca*)	Eucalyptus (*Eucalyptus Camaldulensis*)	Silver Birch (*Betula Verrucosa*)
Cellulose	40	39.5	45	41
Hemicellulose				
Glucomannan	16	17.2	3.1	2.3
Glucuronoxylan	8.9	10.4	14.1	27.5
Other Polysaccharides	3.6	3	2	2.6
Total Hemicellulose	28.5	30.6	19.2	32.4
Lignin	27.7	27.5	31.3	22
Total Extractives	3.5	2.1	2.8	3

1.2 Pyrolysis

Pyrolysis is the thermal decomposition of organic compounds in the absence of an oxidizing agent into vapor and solid compounds. The vapor products are divided into vapors that are condensed into liquid products, and gas products that are not condensed. The liquid products are usually referred to as pyrolysis oil or bio-oil, while the solid products are usually referred to as bio-char. The rate and extent of decomposition depends on the composition of the feedstock, the reactor temperature, the biomass heating rate, and the reactor pressure. At high temperatures, the condensable vapors will undergo secondary cracking reactions to produce gas products [14]. Reaction conditions for typical pyrolysis processes are shown in table 1.2. Typical product yields for typical pyrolysis processes are shown in table 1.3.

Table 1.2 Typical Pyrolysis Reaction Conditions [15-17]

Classification	Biomass Heating Rate Ranges (°C/s)	Typical Reactor Temperatures (°C)	Typical Vapour Residence Times
Slow Pyrolysis	0.01-2	350-400	hours-weeks
Intermediate Pyrolysis	2-10	350-450	10-20 s
Fast Pyrolysis	>1000	450-550	~1 s

Table 1.3 Typical Pyrolysis Product Yields [16]

Product Yield (wt. %) [Dry Basis]	Slow Pyrolysis	Intermediate Pyrolysis	Fast Pyrolysis
Liquid	20-50	35-45	50-70
Solid	25-35	30-40	10-25
Gas	20-50	20-30	10-30

In pyrolysis processes, the biomass heating rate and the vapor residence times are the most important process parameters for determining the product distributions. At high heating rates, biomass solid material rapidly depolymerises to primary volatiles, while the rate of dehydration to stable anhydrocellulose molecules is slow, which results in low solid yields. At low heating rates, the rate of decomposition of the biomass is slower, so the rate of formation of solid anhydrocellulose is much higher [18]. Reed et al. [19] studied the effect of the heat flux of cellulose samples. They found that heating fluxes of 6.3, 46, and 12,500 W/cm^2 resulted in 33, 3, and ~1 wt. % char yields.

During pyrolysis, the heat flux to the biomass is proportional to the temperature difference between the biomass and the reactor, so the biomass heating rate and flux are increased at higher reactor temperatures. The biomass heating rate and flux are also higher for small particles than they are for large particles. At sufficiently high reactor temperatures (usually 450-550 °C) and small biomass particles sizes (< 2 mm), the yield of bio-oil is maximized and the solid yield is minimized [18]. Processes that utilize larger particles have higher solid yields, lower liquid yields, and reduced biomass grinding costs.

The rate of secondary cracking of vaporized liquid products to gas products is also increased at higher reactor temperatures. Raising the reactor temperature above the temperature requirement to remove heat transfer limitations between the biomass and heat transfer medium results in decreased liquid yields. Long vapor residence times result in increased secondary cracking and lower liquid yields. Pyrolysis processes that are designed to maximize liquid yields require low vapor residence times and rapid quenching of the vapors [14].

X-ray Photoelectron Spectroscopy analysis of bio-char particles revealed that a substantial amount of the exposed surface of bio-char contains alkali and alkali earth metals [20], which are known catalysts that promote the cracking of condensable vapors to char and gas products during pyrolysis [21]. For this reason, liquid yields are higher when the char is separated from the vapor stream.

There are currently no large scale production plants producing pyrolysis oils. Several demonstration scale plants have been built utilizing different reactor configurations. Information about the reactor configurations are summarized in table 1.4.

Table 1.4 Pyrolysis Demonstration Scale Plants [22-25]

Reactor Configuration	Largest Proven Capacity (kg/hour)	Typical Liquid Yields (wt. %) [Dry Basis]	Maximum Particle Size Requirement (mm)
Bubbling Fluidized Bed	8000	70-75	2
Circulating Fluidized Bed	4000	70-75	2
Vacuum Pyrolysis	3500	35-50	50
Augur Pyrolysis	2083	43-58	2
Ablative Pyrolysis	2000	70-75	20
Rotating Cone	2000	60-70	5

In fluidized beds, gas is used to cause an upward force on a bed of solid particles sufficient to suspend the particles in a fluid-like state, but insufficient to entrain large portions of the bed. Dried ground feedstock is injected into a fluidized bed of sand particles. The process energy requirements are provided by combusting gases produced during pyrolysis and supplemental natural gas. Heat generated by combustion of the gases is transferred to the fluidized bed by heating coils. The bio-char particles are entrained with the vapor stream and collected in cyclones. The liquid products are condensed after passing through the cyclones [22-23, 26-28]. The maximum scale of bubbling fluidized beds is limited by the amount of heat that can be transferred through the heating coils [27]. The heating coils are also vulnerable to attrition from sand particles [29].

The large scale application of circulating fluidized beds (CFB) (or circulating transport beds) has been industrially proven by fluid catalytic crackers and Fluid Cokers™. CFB reactor configurations utilize a fluidized bed and a burner. The fluidized bed unit in the CFB is operated using most of the principles and configuration utilized in the bubbling fluidized bed, with some major differences. While the bubbling fluidized bed configuration only uses enough fluidization gas to fluidize the bed and entrain the produced char from the bed, CFB configurations utilize enough fluidization gas to entrain a constant flow of sand particles from the reactor (typically at a flowrate 10-20 times the biomass feed rate). The produced char and entrained sand from the fluidized bed are collected in the cyclones. The cyclones transfer the sand and char to the burner, where the produced char is combusted to heat the sand. The heated sand is recirculated back to the reactor. The constant recirculation of sand is used to maintain the fluidized bed at the desired temperature [22-23, 27-28].

In auger reactors dried ground biomass and heat carriers are fed into a horizontal vessel though separate hoppers. Examples of heat carriers that have been used include heated sand, heated steel balls, and heated ceramic balls. Augers force the biomass and carrier medium towards the exit of the vessel. The biomass reacts and the vapor products exit the vessel and are condensed after passing through cyclones. The heat carrier medium exits the end of the vessel and is fed to a burner where the char is combusted to reheat the heat carrier medium. The heated carrier is then recirculated back to the auger reactor [22-24, 27, 30]. The advantages of auger reactors relative to fluidized beds include the reduced capital and operating costs as it does not require fluidization gas, liquid products with negligible solid contamination, and the capability of handling solids that are normally difficult to feed into reactors. The vapor residence times of augur reactors have been shown to be largely independent of the augur rotational speed, which makes the vapor residence time a function of reactor design and geometry, rather than an easily modifiable process variable. Typical vapor residence times for augur pyrolysis are 5-30 seconds. The longer vapor residence times and longer contact times with bio-char result in lower liquid yields and higher char yields than pyrolysis in fluidized beds [22, 24].

In rotating cone configurations, the base of the rotating cone contains an impellor. The impellor forces dried ground biomass onto the heated surface of the rotating cone. The centrifugal force of the rotating of the cone causes the biomass and sand to be mixed and transported up to the tip of the cone. The sand and produced char drop from the cone into a fluidized bed, where they are lifted into a burner where the char is combusted to heat the sand. The hot sand is reintroduced back to the rotating cone. The cone shape minimizes the volume of the gas phase, which reduces the vapor residence time. The main advantages of the rotating cone design relative to fluidized beds is the reduced capital and operating costs as it does not require fluidization gas, the liquid products contain lower concentrations of entrained bio-char, and more flexibility in feedstock sizes. Disadvantages relative to circulating fluidized beds are 5-15 wt. % lower typical liquid yields and the process has not been demonstrated at an industrial scale [22-23, 27-28, 31-32].

Vacuum pyrolysis is typically performed at 450 °C and a total pressure of 100 kpa. Molten nitrate salts are heated to 575 °C using a burner that combusts the gases produced during pyrolysis. Biomass is indirectly heated by the salts, while being mechanically agitated. The process operates at much lower heat transfer rates than fast pyrolysis processes, which results in significantly lowered liquid yields. As high heat transfer rates are not needed, the process accepts significantly larger particle sizes than fast pyrolysis processes, which results in reduced grinding costs. The process does not use fluidization gas, so the liquid products produced through vacuum pyrolysis contain lower concentrations of bio-char contaminants than the liquid products of fluidized beds. The process produces lignin derived fractions with lower molecular weights than the lignin fractions produced through fluidized bed pyrolysis, which could be useful for processes extracting phenolics. While the process does not use expensive fluidization equipment, it is energy intensive and requires high capital cost vessels, solid feeders, and reactor seals needed to be operated at reduced pressures. Making the process viable would require high value extraction from both the bio-oil and solid products to be competitive with fast pyrolysis process due to the higher solid and lower bio-oil yields [22-23, 28, 32-34].

In ablative pyrolysis, dried biomass particles are forced into contact and moved along a heated reactor wall by compression or centrifugal force. The gases and char produced during pyrolysis are combusted to heat the walls of the reactor. The biomass leaves an oily film that evaporates. Liquid vapors are condensed after passing through cyclones to collect char particles. The main advantage of the process is the liquid yield is not limited by heat transfer to the biomass particles, which means the process can accept larger particles and still maintain high liquid yields similar to fluidized bed processes. The process is limited by the amount of heat that can be transferred to the reactor wall, which could be a problem in a scaled-up unit. The process also has the problem of maintaining reactor wall contact with diverse morphologies (particle shape, structure, and density), which limits the types of biomass that can be processed. The process requires either large quantities of motive gas or complex mechanical systems that would add mechanical reliability issues. The viability of the process has not been demonstrated at an industrial scale [22, 25, 27-28].

1.3 Bio-oil

Much like petroleum based oils; bio-oil contains hundreds of identified and an unknown amounts of unidentified compounds. The chemical composition of bio-oils varies depending on the feedstock, reactor configuration, and reactor conditions. The identified compounds in bio-oil can be categorized into acids, alcohols, aldehydes, alkenes, aromatics, esters, furans, guaiacols, ketones, nitrogen compounds, phenols, sugars, syringols, water, and miscellaneous oxygenates [23]. In addition to the identified compounds, bio-oils contain oligomeric species in aerosol form that can’t be detected using gas chromatography. Based off of high pressure liquid chromatography and electrospray mass spectroscopy, the molecular weights of the oligomerics range from several hundred to over 5000 grams/mole. The oligomerics are produced from the fragmentation of lignin during pyrolysis [11]. The chemical composition of some literature bio-oils are summarized in table 1.5.

Table 1.5 Chemical Composition of Literature Bio-oils [35]

	Yield (wt. %) [Wet Basis]				
Chemical Group	Wheat Straw	Switch Grass	Miscanthus	Willow SRC	Beech Wood
Acids	3.58	2.55	2.15	2.73	7.66
Alcohols	5.63	4.44	3.68	4.52	3.30
Aldehydes	6.58	8.04	7.70	7.07	6.30
Esters	2.94	3.32	4.43	2.79	3.69
Ethers	4.84	7.23	5.62	2.78	4.02
Furans	5.41	6.12	4.98	2.77	8.49
Ketones	9.77	7.73	12.94	14.81	10.78
Phenols	16.62	14.86	15.33	24.30	20.80
Water	22.1	21.60	22	15	12.8
Unidentified	22.53	24.12	21.18	23.23	22.17

1.4 Bio-oil Valuation

While most of the work on valuation of bio-oil has been focused on production of fuels, the successful partial replacement of petroleum based feedstocks requires any partial substitute to supply the chemical feedstocks and products used in almost every industry on the planet. This is an ambitious long term goal that would be impractical to implement in the early stages of pyrolysis bio-refinery development. More realistic short term goals would include the focus on the production of select profitable platform chemicals, and the conversion of the remaining bio-oil components into infrastructure compatible fuels. While the decisions on which platform chemicals to focus on are debatable, that topic falls outside the scope of the research in this thesis. For the purposes of the research behind this thesis, the focused platform chemicals were described by Task 42 of the Bioenergy division of the International Energy Agency [36]. An example of list of possible platform chemicals that could be produced from the pyrolysis of biomass is shown in table 1.6.

Table 1.6 Possible of List of Platform Chemicals from Biomass [36-37]

Compound	Compound Type	Source	Boiling Point (°C)
Acetic Acid	Carboxylic Acid	Hemicellulose	118.1
Furfural	Heterocyclic Aldehyde	Hemicellulose	161.6
Levoglucosan	Sugar Intermediate	Cellulose	383.7
Phenolic Compounds	Examples of Phenolic Compounds	Lignin	
Phenol	Phenol	Lignin	181.9
Guaiacol	2-methoxyphenol	Lignin	205.1
Creosol	4-methylguaiacol	Lignin	221.1
Catechol	2-hydroxyphenol	Lignin	245.1
Eugenol	4-allyl-2-methoxyphenol	Lignin	253.3
Syringol	2,6-dimethoxyphenol	Lignin	262.6
Vanillin	4-hydroxy-3-methyoxybenzaldehyde	Lignin	331

Research is ongoing for the extraction of platform chemicals from bio-oil. De Haan et al. [38] developed a process to extract 99.84 wt. % of the acetic acid and > 99 wt. % of glycoaldehyde from the polar aqueous phase of bio-oil using 2-ethylhexanol as a solvent. Žilnik and Jazbinšek [39] performed phenolic extraction studies on the aqueous and organic phases of bio-oil. They concluded the usage of a methyl isobutyl ketone solvent combined with a 0.1-0.5 M NaOH solution was the most efficient of the tested extraction methods with an extraction of 85 wt. % of the phenolics in the bio-oil. Ensyn has a process that extracts speciality food chemicals [22], but the demand for that flavoring is low so it would be unsuitable for mass production.

1.5 Requirements for Conversion of Bio-oil into Usable Fuels

While the processes for the extraction of platform chemicals from bio-oil have not been developed, research needs to continue on developing processes to convert the remaining portions of bio-oil into fuels that are compatible with existing infrastructure. The physical and chemical properties of typical wood based bio-oils are compared to typical values of heavy fuel oil in table 1.7.

Table 1.7 Comparison of Typical Wood Bio-oils and Heavy Fuel Oil Properties [40-41]

Physical Property	Bio-oil	Heavy Fuel Oil
Water (wt. %)	15-35	0.1
pH	2.5	
Density (g/cm^3)	1.15-1.25	0.94
Carbon (wt. %) [Dry Basis]	50-64	85
Hydrogen (wt. %) [Dry Basis]	5.2-7	11
Oxygen (wt. %) [Dry Basis]	35-40	1
Sulfur (wt. %) [Dry Basis]	.05-.3	2.3
Nitrogen (wt. %) [Dry Basis]	.05-.4	0.3
Ash (wt. %)	0-0.2	0.1
HHV (MJ/kg)	16-19	40
Viscosity (cP) at 50°C	40-150	180
Solids (wt. %)	0.2-1	1
Distillation Residue (wt. %)	up to 50	1
Average Molecular Weight (g/mol)	600-700	180-400

The large quantities of water in the bio-oil need to be removed to comply with fuel standards. Large quantities of water in hydrocarbon fuels promote phase separation, corrosion issues in areas susceptible to rust, and emulsions. The bio-oil has lower heating values when compared to petroleum fuel oils. The removal of the water would raise the heating value of the bio-oil, but the dry bio-oil would still have around 40 % lower heating values than listed literature petroleum fuel oil.

The high acidity of bio-oils causes corrosion in materials with less acid resistance than AISI 316 stainless steel [42]. Oasmaa et al. [43] concluded that 60-70 % of the acidity is caused by volatile acids, approximately 20 % is caused by the sugar fraction, 5-10 % caused by phenolics, and 5-10 % is caused by fatty and resin acids. Xu et al. [44] separated the carboxylic acids from the bio-oil, which resulted in the pH of the bio-oil being raised from 2.52 to 5.47. This indicates the acidity problems of bio-oils could be significantly reduced, or perhaps eliminated during volatile acid product extraction steps. The predominant volatile acids in bio-oil are acetic acid and formic acid [43], which have boiling points of 118.1 °C and 100.8 °C.

Increases in the viscosity, surface tension, and/or density of a fuel increases the size of the fuel droplets and changes the spray characterisation of fuel injectors, which significantly affects the vaporization, ignition, and combustion of the droplets [45]. The successful integration of bio-oil into fuel systems would require the integrated fuels to meet existing fuel standards.

The high oxygen content of bio-oils result in high viscosities, immiscibility with petroleum based fuels, thermal instability, and polymerization [46]. In petroleum refineries, the metal and heteroatom (nitrogen, oxygen, and sulfur) contents of petroleum fractions are reduced by various processes including concentration of the contaminants in the distillation residue, concentration into coke, acid treating, and caustic treating. Those processes never completely remove the contaminants from the fractions, so the petroleum fractions have to be treated with hydrogen and catalysts in a hydrotreating or hydrocracking processes to remove contaminates to meet product or feedstock quality standards [47]. The oxygen contents of temperature cuts of literature hardwood bio-oils are shown in table 1.8.

Table 1.8 Oxygen Contents of Temperature Cuts of Literature Hardwood Bio-oils [48]

Boiling Point Range (°C)	BTG (wt. % O)	Dynamotive (wt. % O)	Ensyn (wt. % O)	Pyrovac (wt. % O)
27-87	48.6	46.6	47.2	49.1
Water	88.8	88.8	88.8	88.8
87-127 (dry)	44.9	44	48.4	46.9
127-177	25.2	26.4	22.4	17.8
177-227	7.6	8.6	24.2	14.2
227-285.1	24.5	21.8	24.	26.1
Levoglucosan (386)	49.3	49.3	49.3	49.3
Xilose		53.3		
Cellobiosan	49.3	49.3		49.3
All Components	55.1	48.1	45.6	41.6
All Components –Water	40.4	37.2	34.6	32.8
All Components With Boiling Points > 127 °C	37.7	34.6	31.7	30.5

Water is usually the largest contributor to the high oxygen content of bio-oil. If the water in the bio-oils listed in table 1.8 was removed without affecting the other components, the oxygen contents of the bio-oils would be reduced by 8.8-14.7 wt. %. In the bio-oils listed in table 1.8, 75.4-83.2 wt. % of the molecules in the 27-87 °C temperature cut and 69.8-83.9 wt. % of the non-water molecules in the 87-127 °C temperature cut were composed of molecules with 1-2 carbon atoms. Petroleum refineries do not hydrotreat or hydrocrack 1-2 carbon feedstocks, but one can speculate that hydroprocessing this fraction could result in the consumption of expensive hydrogen and catalysts to convert oxygenated products such as formaldehyde and acetaldehyde into less valuable products such as methane and ethane, which are usually combusted to power refinery operations. If the compounds with boiling points less than 127 °C could be removed from the bio-oils listed in table 1.8 without affecting the other compounds, the water would have been removed from the bio-oils, there would have been an estimated 60-70 % reductions in the acidity of the bio-oils, and the oxygen contents of the bio-oils would be reduced by 11.1-17.4 wt. %.

1.6 Bio-oil Instability

Bio-oils are chemically unstable even at room temperature. The instability is observed as evaporation of volatile compounds, increases in viscosity, and phase separation. Bio-oils contain compounds that can react to form larger molecules. The main observed chemical reactions are polymerization of compounds with double bonds, etherification and esterification between hydroxyl, carbonyl, and carboxyl groups [42]. As bio-oils are aged, the viscosity increases which can be directly correlated to increases in the average molecular weight of the bio-oil. Thus increases in the molecular weight of bio-oils can be used to measure the aging rate of bio-oils [49]. Fratini et al. [50] studied the microstructural characterization of bio-oils that were aged for 3, 6, and 18 months. Fratini et al. concluded that during pyrolysis, partially cracked lignin molecules expel lignin oligomers from the biomass. The oligomers polymerize during storage, until the heaviest lignin rich fraction separates out of the matrix as a viscous sludge [50].

Agblevor et al. showed that over 90% of the remaining char particles in the bio-oil that were not removed by cyclones were less than 1 micron in size [20]. Agblevor et al. [51] showed that the fraction of char fines in the bio-oil had a significant impact on the rate at which viscosity increased during ageing, and concluded the large surface area of exposed alkali metals was responsible for the viscosity increase rate during ageing.

1.7 Distillation of Bio-oil

While the some of the obvious goals of upgrading bio-oil such as the removal of water and volatile acids sound simple and straightforward, the unstable and reactive nature of bio-oils makes separating compounds difficult. Even atmospheric distillation, the most widely used separation process in petroleum refineries around the world cannot be practically performed on bio-oil. When bio-oil is heated to 100 °C or higher, the bio-oil rapidly polymerizes and produces approximately 35-50 wt. % yield of solid residues and a distillate containing the removed water and volatile organic compounds [18, 52]. Integration of bio-oil into petroleum refinery atmospheric distillation units would result in significant unit fouling and the eventual failure of the unit.

Deng et al. [53] managed to successfully distill bio-oil at atmospheric pressure using glycerol as a solvent or diluent to a maximum temperature of 250 °C with a single distillation 83.22 wt. % glycerol recovery. Reusing recovered glycerol for additional 1-2 distillations resulted in 5.8-7.74 wt. % reductions in glycerol recovery in each successive distillation. No data was cited for reusing glycerol in a fourth distillation. It was mentioned that the obtained pyrolytic lignin was slightly polymerized.

Zhang et al. [54] distilled rice husk bio-oil at atmospheric pressure to 240 °C. The solid distillation residues were co-pyrolyzed with fresh rice husk to form bio-oil. The process resulted in acetic acid, propanoic acid, and furfural recovery efficiencies of 88.34, 91.8, and 85.11 wt. %. The effects of using solid distillation residues as a co-processing feed were surprisingly not discussed.

Zheng et al. [55] managed to successfully distill bio-oil at 15 mm Hg to a maximum temperature of 80 °C. When stored for 30 days at °C and 80 days at 20 °C, the viscosities of the distilled bio-oils were not significantly changed. The resulting distilled bio-oils has essentially no water, neutral pH, a 96.33 % increase in heating value, a 75.35 % reduction in the dry basis oxygen content, and an atomic H/C ratio similar to gasoline. Selected physical and chemical properties of the distilled bio-oils are shown in table 1.9.

Table 1.9 Physical and Chemical Properties of Literature Vacuum Distilled Bio-oil [55]

Property	Original Bio-oil	Distilled Bio-oil
H2O (wt. %)	25.2	0.01
pH	2.8	6.8
Density (kg/m3)	1190	1270
LHV (MJ/kg)	17.42	34.2
Flash Point (°C)	76	92
Pour Point (°C)	-18	-10
C (wt. %) [Dry Basis]	55.75	76
H (wt. %) [Dry Basis]	6.52	12.2
O (wt. %) [Dry Basis]	37.33	9.2
H/C (atomic ratio)	1.39	1.91
O/C (atomic ratio)	0.50	0.09
Acetic Acid (wt. %)	4.56	0.36
Formic Acid (wt. %)	7.69	0.6
1,2-Benzenedicarboxylic acid (wt. %)	1.1	0
Benzoic Acid, 3-methyl- (wt. %)	1	0.05
Acetol (wt. %)	2.24	0.21
Levoglucosan (wt. %)	0.92	0.07

1.8 Petroleum Fractionation

A crude distillation unit (CDU) is used to fractionate crude oils at atmospheric pressure into different boiling point fractions. A simplified diagram of a CDU is shown in figure 1.1. The operating temperatures of CDUs and petroleum refinery vacuum distillation units (VDUs) are too high to process bio-oil, so the focus here is placed on the fractions in which bio-oil can be integrated.

Figure 1.1 Simplified Diagram of a Crude Distillation Unit [47, 56-58]

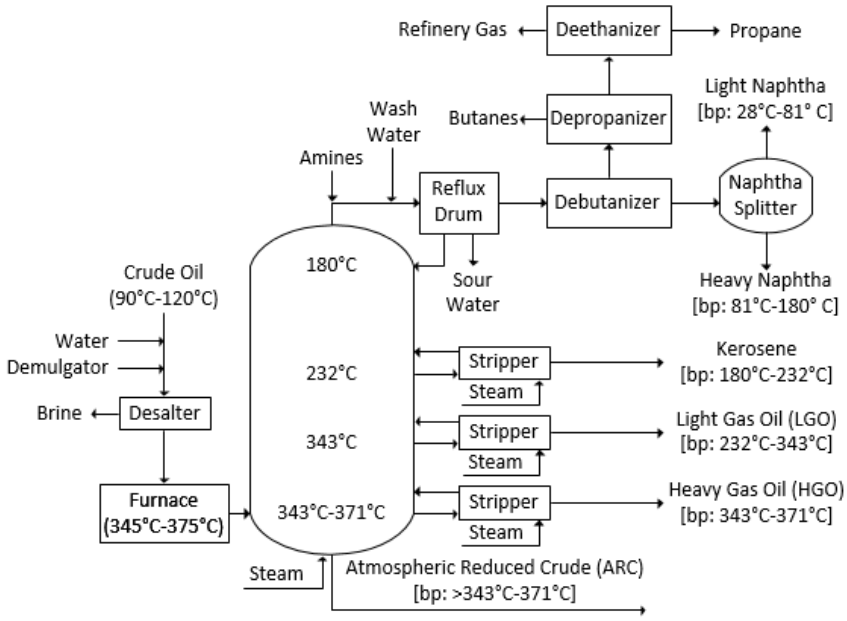

Propane, butane, and isobutane are separated from the rest of the gases, condensed, and sold as liquefied petroleum gas (LPG). The rest of the gases (typically referred to as refinery gas, fuel gas, still gas etc.) are usually combusted to power refinery operations. The light and heavy naphtha fractions are upgraded separately and blended to produce gasoline. The upgraded kerosene fraction is blended into jet fuels and fuel oil. The upgraded light gas oil (LGO) fraction is blended into diesel fuels. The heavy gas oil (HGO) (or atmospheric gas oil) fraction is used as a feedstock for a Fluid Catalytic Cracking (FCC) unit [47, 56-58].

Distillation unit temperature operational limits are based off the temperatures at which the feedstock will decompose. The units are operated below temperatures at which the feedstock would undergo significant cracking, to minimize fouling in the unit. Compounds with boiling points above the flash zone temperature of the distillation unit are referred to as reduced crude, topped crude, residue, and bottoms. As compounds have lower boiling points in reduced pressure environments, the atmospheric reduced crude (ARC) fraction is further fractionated in a vacuum distillation unit operated at 15-100 mmHg and below temperatures at which the ARC would undergo significant cracking.

The main distillate products of VDU are usually vacuum gas oils (VGO), which are blended with HGO and used as a feedstock for FCC units. The remaining compounds with reduced pressure boiling points higher than the flash zone temperature of the VDU are referred to as vacuum reduced crude (VRC), vacuum topped crude, vacuum residue, or vacuum bottoms. VDUs are also capable of processing some types of ARC to distill lubricating oils [47, 56-58].

1.9 Fluid Catalytic Cracking

Fluid catalytic cracking (FCC) units are used to convert HGO, VGO, and coker gas oil feedstocks into naphtha, kerosene, and LGO (the kerosene and LGO are typically reported as light cycle oil [LCO]). Refineries without a coker will also process VRC into the FCC unit after the VRC has been pretreated to remove sulfur and metals. Preheated feed is combined with the liquid recycle stream and contacted with recirculated heated catalysts in a riser. The hot catalysts vaporize the feed. Once the feed is vaporized, the vapor is cracked as it travels up the riser. Coke formed during the cracking reactions is deposited on the catalysts. After passing through the riser, the vapor is separated from the catalysts in cyclones. The liquid products are sent to a fractionating column where the liquid products are separated into product fractions. The coke on the catalyst is combusted in a regenerator to regenerate the catalysts [47, 56-58].

FCC catalysts contain aluminum and silica atoms that are tetrahedrally joined to four oxygen atoms in an acidic zeolite structure, amorphous aluminum which provides larger cracking sites than the zeolite sites, and a binder and filler to maintain structural integrity [59]. The catalysts function by chemisorptions through proton donation and desorption [47]. When compared to thermal cracking, catalytic cracking produces higher yields of gasoline and middle distillates, while producing lower gas yields. The gasoline produced has higher concentrations of alkane isomers and aromatics which raise the octane rating of the gasoline [47].

Vanadium, copper, nickel, and alkali earth metals are FCC catalyst poisons that permanently deactivate various catalyst sites. Nickel and vanadium are also catalysts that promote dehydration reactions, which can remove hydrogen from stable compounds and make unstable alkenes that polymerize into heavier hydrocarbons. Some petroleum nitrogen compounds can react with catalyst acid sites, which lower the catalyst activity until the nitrogen is removed in the regenerator. Feedstocks containing large quantities of these catalyst poisons need to be pretreated before injection into a FCC unit [59].

Lappas et al. [60] co-processed 85 wt. % VGO with a blend of LCO and hydrotreated bio-oil (6.5 wt. % oxygen) in an isothermal riser operated at 520 °C. The co-processed feed produced approximately 1 wt. % more gasoline, more LCO, and 0.5 wt. % higher coke yields when compared to processing VGO. The co-processed yields of LPG were lower. At each catalyst to oil (C/O) ratio, the co-processed feed had approximately 1 wt. % lower conversion than processing VGO. The gasoline produced from the co-processed feed had higher concentrations of aromatic content and lower concentrations of alkanes and alkenes.

Fogassy et al. [61] co-processed 20 wt. % hydrotreated bio-oil (21 wt. % oxygen) with VGO in a fixed bed reactor with FCC catalysts. When compared to processing only VGO, the addition of bio-oil to the feed raised coke and refinery gas yields, while reducing LPG and bottoms yields. The yields for gasoline and LCO were comparable to the processing of VGO. The feed conversion at a C/O ratio of 2.9 was approximately 10 % higher when co-processed with bio-oil. The co-processed feed conversions increased at a slower rate than the conversion of pure VGO. The co-processed feed conversion at a C/O ratio of 5.9 was lower than the VGO feed conversion. Fogassy et al. [61] concluded that the increase in acid site coke formation during co-processing lowered the activity of the acid catalysts, which resulted in a higher proportion of the feedstock undergoing thermal cracking rather than catalytic cracking. The gasoline produced from the co-processed feed had higher concentrations of aromatic content and lower concentrations of alkanes and alkenes.

Mercader [62] co-processed 20 wt. % hydrotreated bio-oil (15.5-28 wt. % dry oxygen) with Long Residue FCC feed and FCC catalysts in a micro-activity test reactor at 520 °C. Co-processing reduced the gasoline (0.5-3.8 %) and LCO (1.2-3.9 %) yields, while increasing the LPG (1.2-1.6 %), coke (0.7-1.3 %), and refinery gas (0.3-0.8 %) yields, while producing 3.9-7.9 % water. The CO and CO_2 yields were always lower than 0.5 wt. %, so the oxygen removed from the liquid products favored water over gas formation. Co-processing raised the required C/O ratio needed for 60 wt. % conversion from 3.1 to 3.4-4.3. Processing 100 wt. % hydrotreated bio-oil required C/O ratios of 12-20.2 to maintain 60 wt. % conversion, while reducing the gasoline (7.8-21.7 %) and LCO (5.9-14.3 %) yields relative to processing 100 wt. % Long Residue feed.

Agblevor et al. [63] co-processed #4350 standard gas oil and 15 wt. % bio-oil produced through catalytic pyrolysis (27.19 wt. % oxygen) in an advanced catalyst evaluation unit at 538 °C using FCC catalysts. The product yields were almost identical to processing standard gas oil, with the co-processing resulting in a 0.4 % increase in gasoline yield and a 0.3 % decrease in coke yield. The yields of LPG and coke increased as the C/O ratio increased, while the yield of LCO decreased as the C/O ratio was increased. The gasoline yield stayed within 43.6-44.9 % over the C/O ratios of 6-9. Agblevor et al. attributed this almost constant gasoline yield to a pseudo steady state where the excess gasoline was converted to LPG at higher conversions.

1.10 Coking

Coking processes are non-catalytic thermal cracking processes that are used to upgrade heavy feedstocks (VRC, heavy oil, natural bitumen) into gas oils suitable for injection into FCC units, while producing naphtha, distillates, coke, and gas**.** By converting the coke precursors in the feedstocks into coke inside the coker, the coke formation in the FCC unit is minimized, which improves FCC product yields and quality. The FCC catalyst poisons and sulfur in the feedstocks are concentrated into the coke. The gas oils have viscosities magnitudes lower than the heavy feedstocks [47, 56-58].

Most coking processes are performed in delayed cokers. In delayed cokers, a furnace is used to heat the feedstock to 485°C-505°C and injected into a coking drum. The liquid residence time in the furnace is kept short to delay the cracking reactions from occurring until the liquid reaches a coking drum. Coke accumulates inside the drum, while liquid and gas products are fed to a fractionator for separation. The heaviest products are recycled into the feed stream, heated, and injected into a coking drum. Full drums are purged with steam, and the coke is removed from the bottom of the drum [47, 56-58].

A simplified version of a Fluid Coker™ is shown in figure 1.2. A Fluid Coker™ has a reactor and a burner. The reactor is a fluidized bed of coke particles. The cracking reactions are endothermic, so the reactor must be continually supplied with heated coke from the burner to maintain the desired reactor temperature. The energy needed for the process is provided by combusting excess coke particles generated in the coking process, which also prevents the accumulation of coke inside the units. Heated coke particles are transferred to the reactor through a riser [47, 56-57].

Figure 1.2 Simplified Diagram of a Fluid Coker™ [47, 56-57]

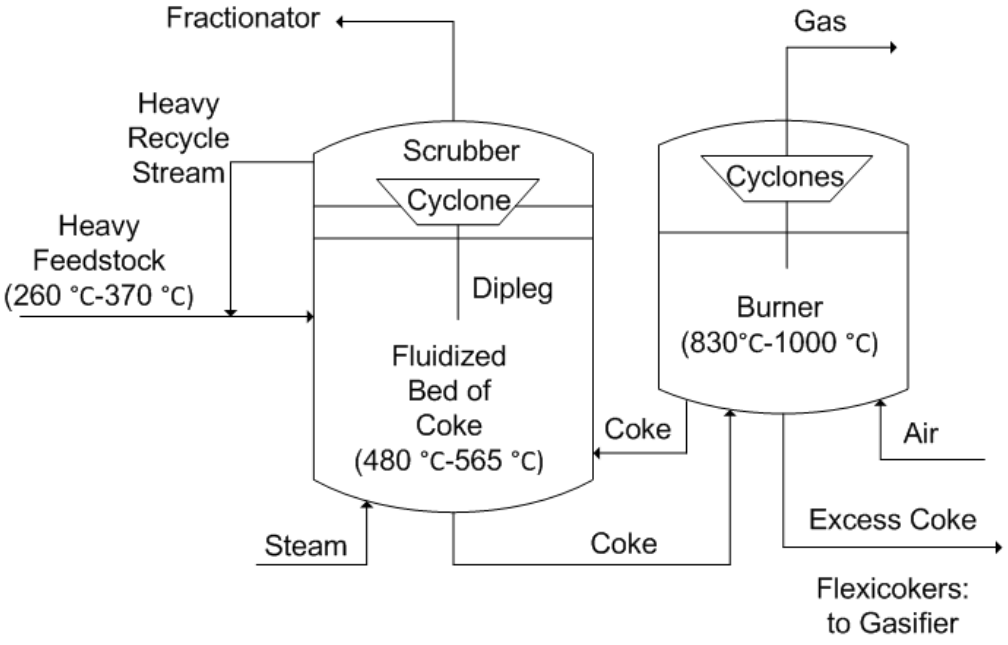

The heavy feedstocks are heated and injected into the fluidized bed where the cracking reactions occur. The vaporized liquid and gas products pass through cyclones, which collects fine coke particles entrained with the exit vapor stream. The vapors enter a fractionator for separation before being condensed. The combination of improved temperature control and the direct injection of feedstock into the reactor allow Fluid Cokers™ to be operated at higher temperatures than delayed cokers. The higher reactor temperatures and better vapour residence time control of Fluid Cokers™ results in lower yields of coke and higher liquid yields [47, 56-57].

The coke formed in fluidized beds has different morphology and physical properties than the coke formed in coking drums. The fluidized beds can't produce manufacturing grade coke for the aluminum or steel industries, which is a major drawback for refineries processing feedstocks capable of producing premium manufacturing grade coke. Fluid Cokers™ are optimally used when the feedstock is only capable of producing fuel grade coke [47, 56-57].

Flexicokers™ have the setup of a Fluid Coker™ with an added gasifier which is used to convert excess coke into a fuel gas. The main advantage of the added gasifier is the fuel gas has low enough sulfur content to be burned without a SO_2 removal system. The fuel gas is also a more flexible fuel than fluid coke [47, 56-57, 64].

ExxonMobil has applied for a patent for the process of co-processing bio-oil with heavy petroleum feedstocks in cokers [65]. ExxonMobil found that the generation of free radicals from the pyrolysis of lignin increased the drying rate of the coke. The increased drying rate reduced the fouling of the stripper section, which increased coker throughput. The coke produced from bio-oil alkali metal compounds in delayed cokers was found to have a lower density and higher porosity relative to coke produced in delayed cokers using heavy oil or natural bitumen feedstocks. In Flexicoking™ processes, the alkali metals in the bio-oil acted as catalysts in the gasifier.

1.11 Research Objectives

The objective of this thesis was to investigate whether the co-pyrolysis of bio-oil with atmospheric reduced crude (ARC) in a novel mechanically fluidized reactor (MFR) would result in increased compatibility of bio-oil with conventional fossil fuel streams. The bio-oil was distilled with ARC to remove the aqueous fraction, and the resulting distillation residues were pyrolyzed in a MFR to determine the difference in product yields and quality compared to those obtained by the co-pyrolysis of untreated bio-oil and ARC. In both cases, the effects of the reactor temperature and the mixing ratios of bio-oil and ARC on the product yields and quality were also investigated.

This thesis has five chapters. The first chapter introduces the subject matter relevant to the thesis and cites the relevant literature for integrating bio-oil into a petroleum refinery. In chapter 2, the experimental apparatus, chemicals, and methodology used in the research are presented.

Chapter 3 describes and discusses the investigation into the effects of co-pyrolyzing raw bio-oil and ARC in a MFR. Chapter 3 of this thesis also describes and discusses the investigation into the effects of the removal of the aqueous phase of bio-oil before co-pyrolysis with ARC. Chapter 4 presents the important conclusions of this study. Recommendations for future work are included in chapter 5.

Chapter 2: Materials and Methods

2.1 Experimental Setup and Procedure

The experimental setup used in this study is shown in figure 2.1. The central unit of the setup was a mechanically fluidized reactor (MFR), which is shown in more detail in figures 2.2-2.3. The MFR had a 0.089 m internal diameter and a height of 0.127 m. The higher viscosity atmospheric reduced crude (ARC) and distillation residue feedstocks were injected into the MFR using a higher pressure variant New Era Pumps Inc. NE-1010 syringe pump. The lower viscosity raw bio-oil was injected into the MFR using a New Era Pumps Inc. NE-300 Just Infusion^{TM} syringe pump. The MFR effluent pipe was connected to a 259 cm^3 heated char filter used to prevent solid particles entrained with the vapor products from entering the condensing train. The heated char filter is shown in more detail in figure 2.4. The heated filter was connected to a condenser used to condense and collect most of the liquid products. The condenser was connected to an electrostatic precipitator (ESP) with a 12.95 kV voltage applied to its electrode, which coalesced and collected fine droplets in the carrier gas leaving the condenser. The ESP was connected to a cotton filter, which was used to check the efficiency of the condensation train.

In all experiments, 450 g of fresh Opta Minerals Inc. Barco silica sand with a sauter mean diameter of 223.4 μm was used as the bed material. Experiments were performed at constant reactor freeboard and filter temperatures of 480, 500, and 530 °C. The initial bed temperatures were 15-18 °C higher than the freeboard temperatures. The MFR was heated using two OMEGA Engineering Inc. 900 W ceramic radiant heaters. The char filter was heated to the freeboard temperature of the MFR using two OMEGA Engineering Inc. 850 W ceramic radiant heaters. The MFR was equipped with an agitator, which mixed the sand into a pseudo fluidized state. The agitator also improved the wall to bed heat transfer. The agitator speed was maintained at 100 RPM, which was found to be the critical value for agitator speed in the MFR during the pyrolysis of ARC, where no further speed increases improved the liquid-solid contact [66].

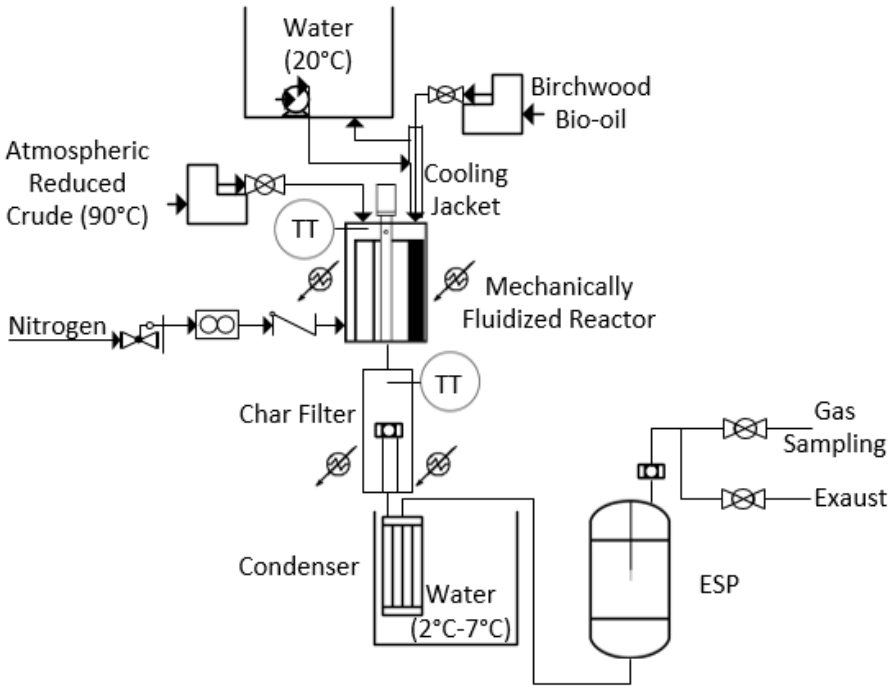

Figure 2.1 Experimental Setup

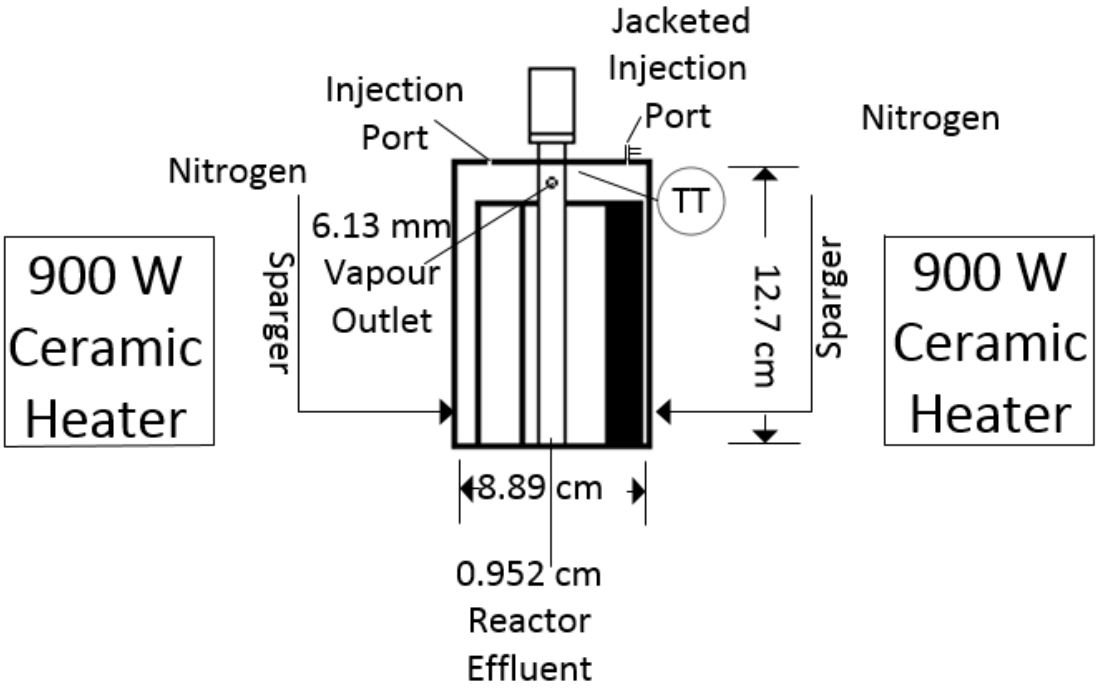

Figure 2.2 Front View of a Mechanically Fluidized Reactor

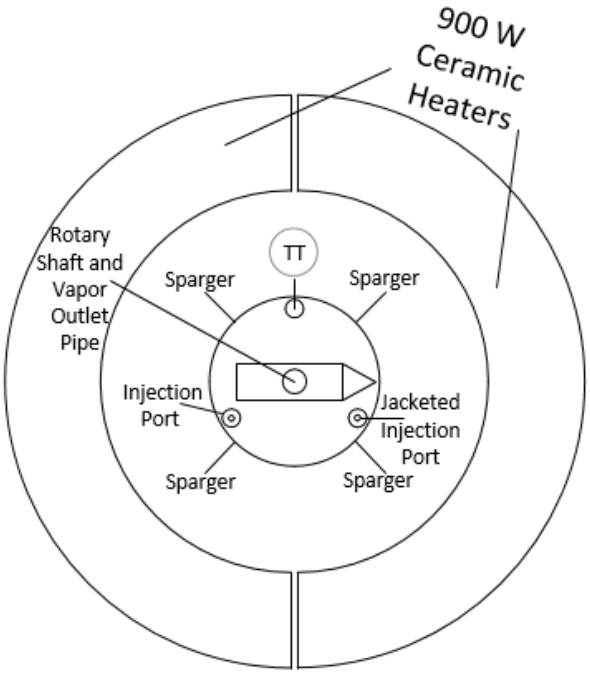

Figure 2.3 Top View of a Mechanically Fluidized Reactor

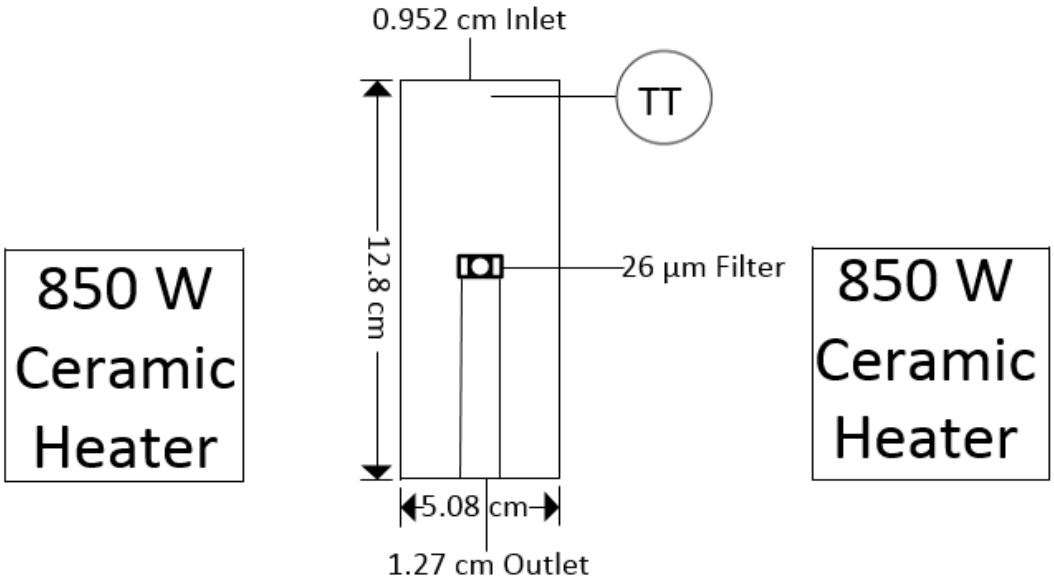

Figure 2.4 Heated Char Filter

The residence time of vapor in the reactor was controlled by constant injection of nitrogen gas through four single hole sparger tubes with inner diameters of 1.49 mm located at 90° intervals. The nitrogen flowrate into the reactor was controlled using an Omega Engineering Inc. FMA-A2308 mass flowmeter. The accuracy of the flowmeter was confirmed using liquid displacement and gas bag volume tests. The estimated initial vapor residence times with an average ARC feed rate of 4 mL/min were 11.9 seconds in the MFR and 4.7 seconds in the char filter.

The injection line used for ARC and distillation residues had an inner diameter of 1.92 mm, while the raw bio-oil feeding line had an inner diameter of 1.2 mm. The injection lines were made of 316 stainless steel. The injection port for raw bio-oil was cooled using a double pipe cooling jacket through which water at 20 °C was circulated continuously in order to prevent the temperature of the feeding line from rising to the point where bio-oil would crack inside the feeding line. The heavy feedstock injection port and the raw bio-oil injection port were 6.6 cm apart.

The liquid and solid yields in the experiments were determined by gravimetric analysis and the gas yields were calculated by differences in the mass balance. The liquid yields were obtained from the weight differences of the feedstock injection lines, the condenser, the ESP, and the tube connecting the condenser to the ESP before and after the experiments. The solid yields were obtained from the weight differences of the MFR and char filter before and after the experiments. In the experiments that used raw bio-oil as at least one or the only feedstock, the liquid products were contaminated by entrained char particles. In those experiments, the collected liquid products were physically separated from the char with a centrifuge. The mass of char in the liquid products was subtracted from the liquid mass balance and added to the solid mass balance. The liquid products produced from the pyrolysis of ARC or distillation resides did not contain any detectable solids.

2.2 Co-pyrolysis of ARC and Raw Bio-oil

2.2.1 Feedstocks

The ARC used in the experiments was supplied by Imperial Oil. Based off of boiling point experiments, the lowest boiling compounds were located between 340-350 °C. The raw bio-oil was produced from the pyrolysis of ground birchwood bark at 400 °C in a 58.2 L continuous mechanically fluidized reactor. Ethanol was added to the bio-oil with a concentration of 1.95 wt. % to reduce the aging rate of the bio-oil as described by Oasmaa et al. [67], while maintaining low enough concentrations of ethanol that the physical and chemical properties would not be significantly changed. The elemental composition and physical properties of the feedstocks are summarized in table 2.1.

Table 2.1 ARC and Raw Bio-oil Elemental Composition and Physical Properties

Feedstock	ARC	Birchwood Bio-oil
Water (wt. %)	0	33.69
Carbon (dry wt. %)	85.8	41.6
Hydrogen (dry wt. %)	10.9	6.9
Oxygen (dry wt. %)	3.5	51.4
Sulfur (dry wt. %)	2.2	< 0.1
Nitrogen (dry wt. %)	0.3	0.1
HHV (kJ/g)	42.84	17.37
Viscosity (cP) at 50 °C	400.4	1.19
Density (g/cm^3)	0.94	1.04

2.2.2 Feedstock Preparation and Experimental Procedure

ARC was preheated to 90 °C to reduce the ARC viscosity, and loaded into plastic 60 mL syringes and injected into the MFR using a NE-1010 syringe pump. Raw birchwood bio-oil with 1.95 wt. % ethanol stored at 4°C was loaded into plastic 60 mL syringes and injected into the MFR using a NE-300 syringe pump. Table 2.2 lists the volumetric flowrates the syringe pumps were programmed to input at each mixing ratio.

Table 2.2 Programmed Volumetric Flowrates

Bio-oil in Reactor Feed (wt. %) [Dry Basis]	ARC Volumetric Flowrate (mL/min)	Bio-oil Volumetric Flowrate (mL/min)
0	4	0
24	3	1.3
42	2.3	2.3
100	0	5.4

The inputted volumetric flowrates were designed to maintain a constant dry mass flowrate of 3.76 g/min at every mixing ratio. In practice the feedrate of ARC did not remain constant during the experiments, which resulted in standard deviations of 1.82 and 1.22 dry wt. % bio-oil in reactor feed at the 24 wt.% and 42 wt.% intermediate points. The process parameters used in this study are shown in table 2.3.

Table 2.3 Co-pyrolysis of ARC and Raw Bio-oil Process Parameters

Freeboard and Filter Temperature (°C)	480	500	530
Initial Bed Temperature (°C)	498	515	547
Nitrogen Flowrate (g/s)	0.0159	0.0153	0.0145
Estimated Vapour Residence Time in MFR (s)	11.9	11.9	11.8
Estimated Vapour Residence Time in Filter (s)	4.7	4.7	4.6
Estimated Hot Vapour Residence Time (s)	16.6	16.6	16.4
Initial Reactor and Filter Pressure	Atmospheric		
MFR Mixer RPM	100		
ARC Preheat Temperature (°C)	90		
Oil Injection per Experiment (g) [dry basis]	53-56		
MFR Volume (L)	0.77		
Sauter Mean Diameter of Silica Sand (μm)	223.4		
Mass of Silica Sand (g)	450		

This study investigated the pyrolysis of ARC, the pyrolysis of raw bio-oil, and the co-pyrolysis of ARC and raw bio-oil. The yields and quality of the obtained products were used to determine whether there was any interaction when ARC and bio-oil were co-pyrolyzed, and how the co-pyrolysis affected the product yields and quality.

2.2.3 Liquid Product and Solid Separation Procedure

The pyrolysis of ARC produced single phase liquid products with no detectable solids. The pyrolysis of the raw bio-oil produced single phase liquid products that contained entrained solids. The liquid products of the co-pyrolysis of ARC and bio-oil contained an aqueous phase, and organic phase, and entrained solids. The liquid products produced from the co-pyrolysis of ARC and bio-oil were centrifuged in 45 mL plastic vials for 30 minutes at a frequency of 5500 RPM using a Thermo Scientific Sorvall™ Legend™ X1 centrifuge with a Fiberlite™ F15-6x100y fixed-angle rotor. This resulted in phase separations due to differences in their densities. The aqueous phases were collected using transfer pipettes, the organic phases were collected by pouring the liquid out of the vial, and the solids remained stuck at the bottom wall of the centrifuge tubes.

The high heating values, moisture content, and viscosities of the liquid products were determined for both the aqueous and organic phases. Reported values for the combined product were mathematically calculated based on the weight fractions of the aqueous and organic phases.

2.2.4 Experimental Errors

The pyrolysis of raw bio-oil and the co-pyrolysis of ARC with raw bio-oil resulted in significant tar formation on the char filter mesh. The MFR was not built to be pressurized, so prolonged operation would result in reactor pressure build up until the rotary seal failed and vapor leaked out of the reactor. For this reason, only 53-56 g of organic feedstock was injected per experiment. When loaded with sand, the MFR had a mass of approximately 7.61 kg. Gravimetric analysis of the solid formation in the MFR required a scale that was rated for ±0.5 g accuracy. As the expected solid yields from the process were around 4.2-5.2 g ± yield changes from using bio-oil, the low accuracy of the scale added significant error to the solid and gas yields. As the mass of injected feedstock and liquid product yields were determined using a scale rated for ±0.01 g accuracy, the gravimetric errors in the total liquid yields were negligible.

Experiments that utilized raw bio-oil as the sole or co-feedstock resulted in fine solid contamination of the entire liquid product collection train. Whenever possible, the solid products were scraped from the condenser and ESP, and added to the solid mass balance. Product mass in the condenser, ESP, and plastic connecting tube which could not be manually recovered without the addition of product contaminating solvents were assumed to have solid/liquid contamination ratio consistent with the recovered liquid and solid products. This assumption added experimental error to the mass balances. The unrecovered liquid products from the experiments co-pyrolyzing ARC and untreated bio-oil were assumed to have physical and chemical properties identical to the analyzed organic fraction. This assumption added experimental error, but it is a reasonable assumption to exclude aqueous phase liquid properties from the uncollected liquid as the collection efficiency of the less viscous aqueous phase was significantly higher than the aqueous phase.

Any errors in reported liquid organics yields, water yields, and liquid properties of experiments co-pyrolyzing ARC and raw bio-oil were most likely due to any experimental errors accumulated during bio-oil sampling, pyrolysis temperature control, product collection, phase separation, phase analysis, and mathematical recombination of the separate values to determine values of the original product. While the quantification of experimental error would be impossible, the separation and recombination resulted in reproducible liquid product analyses that were not possible when analyzing liquid products with phase separation.

2.3 Pyrolyzed Distillation Residues

2.3.1 Feedstock Preparation and Experimental Procedure

The feedstocks used in this study were ARC and two distillation residues formed by co-distilling ARC and raw birchwood bio-oil. The properties of the ARC and bio-oil are described in section 2.2.1. The distillation apparatus is shown in figure 2.5.

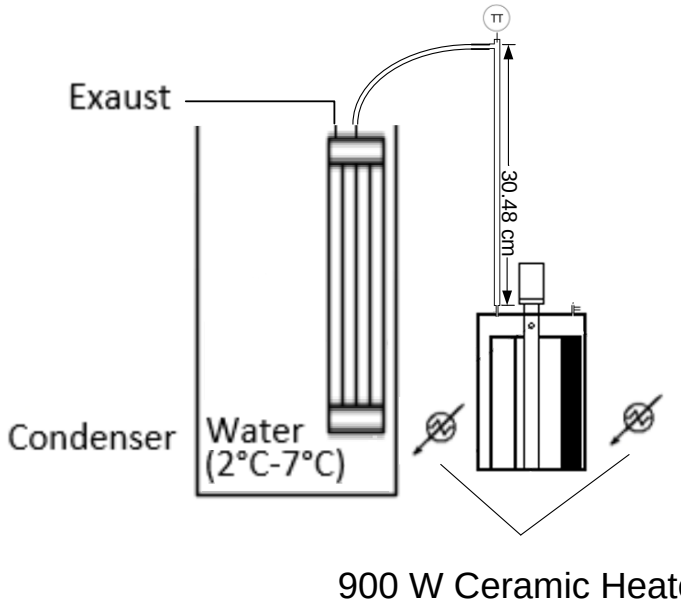

Figure 2.5 MFR Distillation Setup

The MFR was loaded with ARC and raw birchwood bio-oil in the mass ratios of 67:33 and 51:49. The mixtures were heated from ambient temperature to 130 °C. The speed of the MFR agitator was set at 33 RPM for improved heat transfer and mixing. A tube was attached as a vapor outlet at the top of the MFR, which acted as a reflux to increase the separation efficiency of the process. At reactor temperatures below 90 °C, the temperature of the reflux column was maintained approximately 15 °C below the reactor temperature. At reactor temperatures above 90 °C, the temperature difference was maintained between 5-10 °C. The lighter components exiting the reflux tube were condensed and collected in a condenser. The collected distillate was rejected and the remaining residue in the MFR was used as the feedstocks for this study. The inputs and results of the distillations are shown in table 2.4. The measured elemental composition and high heating values of the feedstocks used for this study are shown in table 2.5.

Table 2.4 Distillation Inputs and Results

Feedstock	Residue 19	Residue 29
ARC Input (g)	389.16	327.78
Bio-oil Input (g)	191.59	316.08
Bio-oil Before Distillation (wt. %) [Wet Basis]	32.99	49.09
Weight Difference After Distillation (g)	100.12	181.93
Bio-oil After Distillation (wt. %)	19.05	29.03
Bio-oil Distilled Off (wt. %)	52.19	57.58

Table 2.5 Feedstock Elemental Composition and High Heating Values

Feedstock	ARC	Residue 19	Residue 29
Water (wt. %)	0	0	0
Carbon (wt. %)	85.8	84.6	77.9
Hydrogen (wt. %)	10.9	10.6	9.8
Oxygen (wt. %)	3.5	4.3	6.5
Sulfur (wt. %)	2.2	2.2	1.5
Nitrogen (wt. %)	0.3	0.3	0.8
HHV (kJ/g)	42.84	41.63	37.94

The two distillation residues contained 19 and 29 wt. % bio-oil. Based off the oxygen elemental analysis of the ARC and residues, the bio-oil in residue 19 was estimated to contain 7.95 wt. % oxygen, while the bio-oil in residue 29 was estimated to contain 13.86 wt. % oxygen. As a comparison, the volatile free bio-oil Zheng et al. [55] produced through vacuum distillation contained 9.2 wt. % oxygen. The moisture contents of the ARC and distillation residues were determined by Karl Fisher volumetric titration. The results of the titrations indicated the samples contained 0.12-0.24 wt. % water. The detected water was consistent with atmospheric contamination of anhydrous reagents, and ignored in water calculations. The distillation residues were viscous single phase mixtures without any detectable solid residues. The distillation residues were pyrolyzed using identical reactor conditions used for the pyrolysis of ARC at that specific reactor and freeboard temperature. The distillation residues were heated to 90 °C to reduce the feed viscosity, loaded into plastic 60 mL syringes, and injected into the MFR at a volumetric flowrate of 4 mL/min using a NE-1010 syringe pump.

The yields and quality of the products obtained from the pyrolyzed residues were compared to yields and quality of the products obtained from the pyrolysis of ARC and the co-pyrolysis of ARC and raw bio-oil. The process parameters used in this study are shown in table 2.6. Experiments were also performed at a freeboard temperature of 530 °C. These experiments were performed at a much later time than the experiments at 480-500 °C, and feedstock consistency issues occurred in the time gap between experiments. The feedstocks injected at 530 °C had much higher quantities of ARC molecules and less bio-oil molecules when compared to the experiments at 480-500 °C. The experiments at 530 °C were omitted from this study for this reason.

Table 2.6 Pyrolysis of Distillation Residue Process Parameters

Freeboard and Filter Temperature (°C)	480	500
Initial Bed Temperature (°C)	498	515
Nitrogen Flowrate (g/s)	0.0159	0.0153
Estimated Vapour Residence Time in MFR (s)	11.9	11.9
Estimated Vapour Residence Time in Filter (s)	4.7	4.7
Estimated Hot Vapour Residence Time (s)	16.6	16.6
Initial Reactor and Filter Pressure	Atmospheric	
MFR Mixer RPM	100	
Feedstock Preheat Temperature (°C)	90	
Feedstock Flowrate (mL/min)	4	
Oil Injection per Experiment (g)	53-56	
MFR Volume (L)	0.77	
Sauter Mean Diameter of Silica Sand (μm)	223.4	
Mass of Silica Sand (g)	450	

2.3.2 Liquid Product and Solid Separation Procedure

All the liquid products formed in this study contained a single liquid phase with no detectable solids, so the no product separation procedure was used in this study.

2.3.3 Experimental Errors

The pyrolysis of the methoxy-phenol containing distillation residues resulted in significant tar formation on the char filter mesh. The MFR was not built to be pressurized, so prolonged operation would result in reactor pressure build up until the rotary seal failed and vapor leaked out of the reactor. For this reason, only 53-56 g of organic feedstock was injected per experiment. When loaded with sand, the MFR had a mass of approximately 7.61 kg. Gravimetric analysis of the solid formation in the MFR required a scale that was rated for ±0.5 g accuracy. As the expected solid yields from the process were around 4.2-5.2 g ± yield changes from the bio-oil in the distillation residues, the low accuracy of the scale added significant error to the solid and gas yields.

Any errors in reported liquid organics yields, water yields, and liquid properties of experiments pyrolyzing ARC or distillation residues were most likely due to any experimental errors accumulated during feedstock sampling, pyrolysis temperature control, product collection, and product analyses.

2.4 Liquid Product Analysis Procedures

2.4.1 Liquid Product Moisture Analysis

The feedstocks and liquid product moisture contents were measured using a Mettler Toledo V20 Volumetric KF Titrator using an AquaStar CombiSolvent Keto titrant.

2.4.2 Liquid Product Elemental Analysis

The carbon, hydrogen, sulfur, and nitrogen contents of the feedstocks and liquid products were measured using a FlashEA CHNS elemental analyzer. The sulfur contents of wood based bio-oils are typically in the range of 60-500 ppm [40], which is lower than the 0.1 wt. % detection limit of the elemental analyzer. For this reason, the sulfur content of the bio-oil and liquid products of the pyrolysis of bio-oil were not detectable. The

results for the nitrogen analysis were inconsistent and not reproducible, which is consistent with low nitrogen feedstocks as explained by Oasmaa et al. [67].

The oxygen content of the organic fractions of liquid products was measured using a FlashEA oxygen elemental analyzer. The oxygen content of aqueous fractions of liquid products was calculated by difference of the carbon, hydrogen, nitrogen, and sulfur contents as the FlashEA oxygen analysis of aqueous phases did not result in consistent results. Calculating oxygen content by difference is standard practice in reporting elemental analysis of bio-oils, but even after an extensive literature search no literature explanation was found for why this practice is standard practice.

Equation 2.1 was used to determine the carbon, nitrogen, and sulfur composition of the liquid sample on a dry basis. Equation 2.2 was used to determine the elemental hydrogen content of the liquid sample on a dry basis. Equation 2.3 was used to determine the elemental oxygen content of the liquid sample on a dry basis.

$$\text{Element(dry wt.\%)} = \frac{\text{Element(wet wt.\%)}}{1 - \frac{\text{wt.\% } H_2O}{100}} \quad \text{.....(2.1)}$$

$$\text{Hydrogen(dry wt.\%)} = \frac{\text{Hydrogen(wet wt.\%)} - 0.11189 * \text{wt.\% } H_2O}{1 - \frac{\text{wt.\% } H_2O}{100}} \quad \text{.....(2.2)}$$

$$\text{Oxygen(dry wt.\%)} = \frac{\text{Oxygen(wet wt.\%)} - 0.88811 * \text{wt.\% } H_2O}{1 - \frac{\text{wt.\% } H_2O}{100}} \quad \text{.....(2.3)}$$

2.4.3 Liquid Product High Heating Values

Liquid product high heating values were measured using an IKA C 200 bomb calorimeter. Dry basis calculations were calculated using equation 2.4.

$$\mathrm{HHV(dry)} = \frac{\mathrm{HHV(wet)}}{1 - \frac{\mathrm{wt.\%\ H_2O}}{100}} \quad \text{.....(2.4)}$$

2.4.4 Liquid Product Densities and Viscosities

Liquid product densities and viscosities were measured using an Anton Paar SVM 3000 Stabinger viscometer. It measured the dynamic viscosity and density of the samples according to ASTM D7042. The viscometer automatically calculated the kinematic viscosities of the samples using a method consistent with ISO 3104 or ASTM D445.

2.5 Gas Analysis

The mole fractions of the gas products were measured using a Varian CP-4900 micro gas chromatogram with three thermal conductivity (TCD) detectors. The carrier gas was helium, which prevented proper quantification of hydrogen in the gas. The system was calibrated for butane, carbon monoxide, ethane, ethylene, hydrogen, methane, nitrogen, pentane, propane, and propylene.

The mole/volume fractions of the gases were calculated by normalizing the GC results after subtracting out the nitrogen and hydrogen. The mole fractions were converted to mass fractions using the molecular weights of the individual compounds.

The mole/volume fractions of the simulated refinery gases were calculated by normalizing the GC results after subtracting out the nitrogen, hydrogen, propane, propylene, butane, and pentane. The mole fractions were converted to mass fractions using the molecular weights of the individual compounds. The higher heating values of simulated refinery gases were calculated using the Upper Wobbe Index for each gaseous component [68].

Chapter 3: Results and Discussion

Experimental Results

3.1.1 Liquid Yields from the Pyrolysis of ARC

The liquid yields of the pyrolysis of ARC were 85.6 wt. % at 480 °C, 80.8-81.0 wt. % at 500 °C, and 69.4-73.8 wt. % at 530 °C. The liquid product mixtures formed in single organic phases. Raising the reactor temperature increased the rate of secondary cracking reactions, which resulted in lower liquid yields and higher gas yields.

When the reactor freeboard temperature was increased, the liquid yields decreased by 0.23-0.39 wt. %/°C increase in freeboard temperature. If the 69.4 wt. % liquid yield data point at 530 °C is omitted, the liquid yields decreased by 0.23-0.24 wt. %/°C increase in freeboard temperature. As a comparison, when the fluidized bed temperature of a Fluid Coker^{TM} is increased, the liquid yields typically are reduced by 0.2 wt. %/°C increase in bed temperature [47]. Subsequent experiments utilizing an MFR equipped with a thermocouple capable of measuring the bed temperature indicated the bed temperatures were 15-18 °C higher than the freeboard temperatures.

3.1.2 Liquid Yields from the Pyrolysis of Raw Birchwood Bio-oil

The liquid products from the pyrolysis of raw birchwood bio-oil formed in aqueous solutions. The liquid yields were 66.5 wt. % at 480 °C, 70.5 wt. % at 500 °C, and 72.0 wt. % at 530 °C. If the moisture analyses were accurate, the water yields were 46.6 wt. % at 480 °C, 49.2 wt. % at 500 °C, and 54.2 wt. % at 530 °C. As the bio-oil feedstock contained 33.7 wt. % water, 19.5-30.9 wt. % of the organic bio-oil compounds formed water. The water was probably produced from a combination of cracking reactions during pyrolysis and water forming reactions with unstable liquid products in the condenser. The liquid products contained significant amounts of entrained char particles, which may have promoted ageing reactions that would form water [45].

3.1.3 Product Yields from the Co-pyrolysis of ARC and Raw Birchwood Bio-oil

The co-pyrolysis of ARC and raw birchwood bio-oil produced liquid products in two phase mixtures of an aqueous phase and an organic phase. The aqueous phase yields on a basis of the mass of bio-oil injected are shown in figure 3.1

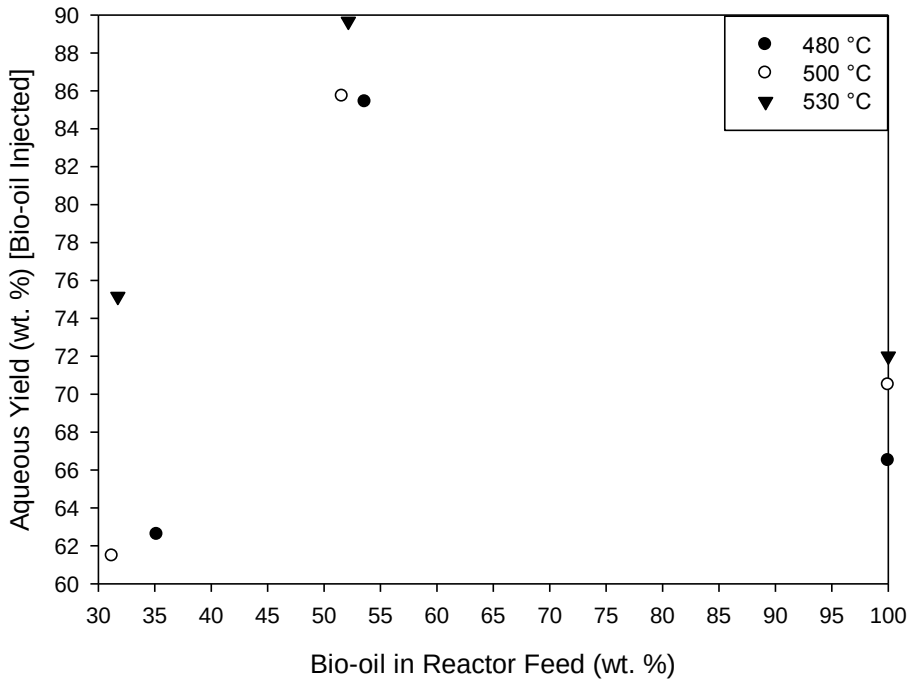

Figure 3.1 Aqueous Phase Yields from the Co-pyrolysis of ARC and Bio-oil

The moisture contents of the aqueous and organic phases were measured by Karl Fischer titration. The moisture analyses of the liquid product phases are discussed in section 3.3.1. The water yields on a basis of the mass of bio-oil injected are shown in figure 3.2. If the 82.6-88.7 wt. % yield points are omitted, the water yields on a basis of bio-oil injected were 14.3-23.2 wt. % higher than the water yields at the corresponding 100 wt. % yield at that temperature. As the organic hydrogen content of the ARC was significantly higher than the bio-oil, ARC molecules would act as hydrogen donors when co-pyrolyzed with bio-oil to promote water formation with organic oxygen. This behavior is consistent with the co-pyrolysis of lignin with formic acid as a hydrogen donor [69].

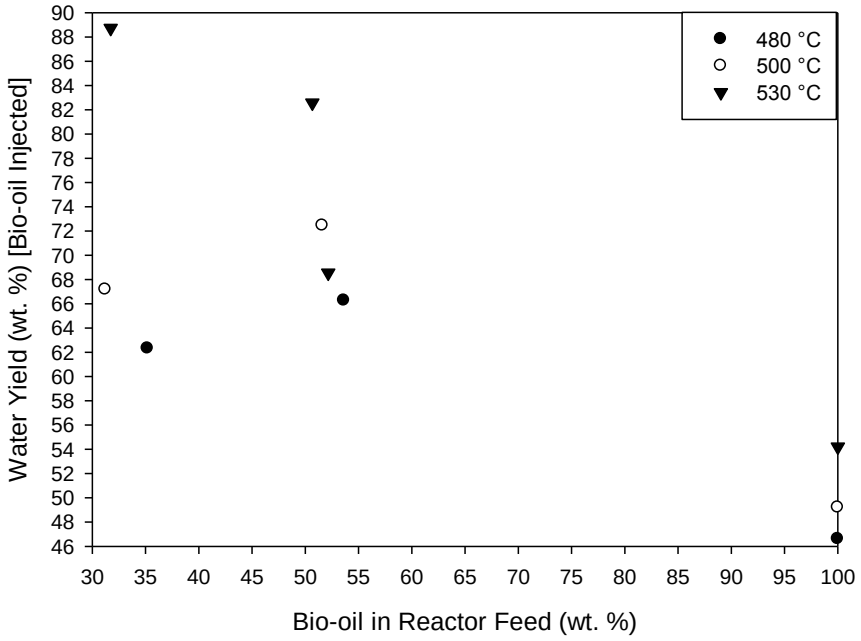

Figure 3.2 Water Yields from the Co-pyrolysis of ARC and Bio-oil

As the bio-oil contained 64.0 wt. % oxygen, the maximum theoretical water yield if all the oxygen was converted to water would have been 72.1 wt. % of the injected bio-oil. As the liquid and gas products contained other oxygenated compounds, the water yields were overstated due to experimental errors. The bio-oil basis aqueous yields at the 51.6-53.6 wt. % mixing ratios were notably higher than the 31.2-35.2 wt. % mixing ratios, which suggests there were significant errors in the liquid yield distribution between the aqueous phases and the organic phases.

The dry basis organic phase yields on a basis of dry mass injected are shown in figure 3.3. When ARC in the reactor feed was replaced with bio-oil, the ratios of dry organic phase yield reductions per wt. % dry bio-oil in the reactor feed were 0.758-0.813 at 480 °C, 0.815-0.937 at 500 °C, and 0.448-0.923 at 530 °C. The average ratios of dry organic phase yield reductions per wt. % dry bio-oil in the reactor feed were 0.786 at 480 °C, 0.876 at 500 °C, and 0.699 at 530 °C. There was very little integration of bio-oil into the organic phase. The bio-oil primarily contributed to the aqueous phase yields.

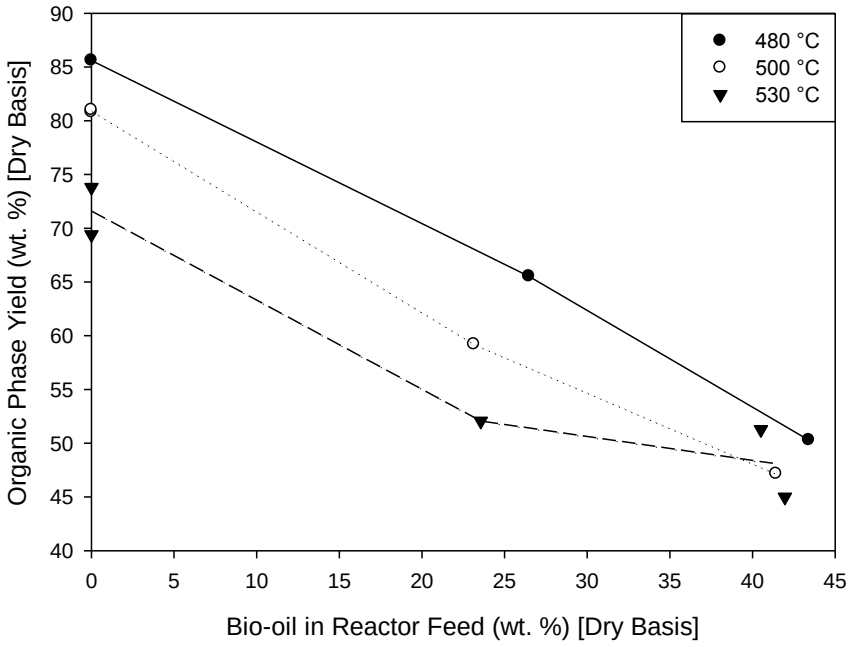

Figure 3.3 Dry Organic Phase Yields from the Co-pyrolysis of ARC and Bio-oil

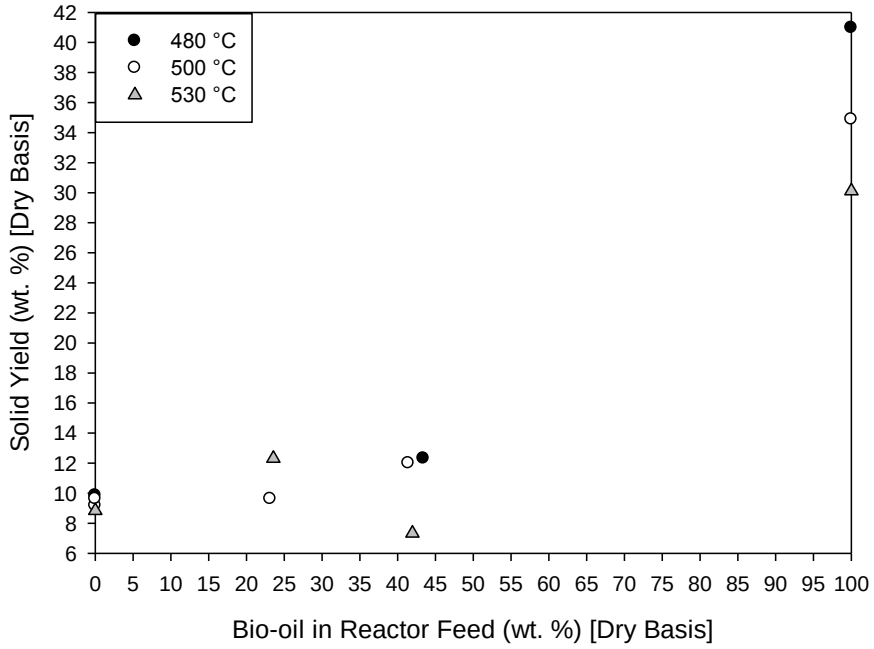

Figure 3.4 Solid Yields from the Co-pyrolysis of ARC and Bio-oil

The dry basis solid yields from the pyrolysis of ARC and raw bio-oil are shown in figure 3.4. The solid yields from the pyrolysis of ARC were 9.8 wt. % at 480 °C, 9.2-9.6 wt. % at 500 °C, and 8.8 wt. % at 530 °C. The solid yields from the pyrolysis of bio-oil were 41 wt. % at 480 °C, 34.9 wt. % at 500 °C, and 30.1 wt. % at 530 °C. The solid yields from the co-pyrolysis of ARC and bio-oil were 7.3-12.3 wt. %.

The solid yields from the co-pyrolysis of ARC and bio-oil were significantly less than the solid yields from the pyrolysis of bio-oil. There is insufficient data to how the co-pyrolysis of bio-oil with ARC would affect the solid and gas yields relative to the pyrolysis of ARC as the solid yields were contradictory. There were results showing yield increases, yield decreases, and no change in yields relative to the pyrolysis of ARC.

Hydrogen transfer plays a key role in cracking processes. Hydrogen deficient hydrocarbons will form coke during thermal cracking processes [70]. Any hydrogen molecules transferred to organic oxygen molecules to form water would not be available to stabilize hydrogen deficient organic molecules. The pyrolysis of raw bio-oil would reduce the bio-oil already low dry H/C ratio to an even lower value. This would explain the high solid yields when pyrolyzed by itself. It is known that co-feeding hydrogen donors with bio-oil will reduce the yield of bio-char produced during cracking [71]. This could explain the low co-pyrolysis solid yields relative to the pyrolysis of raw bio-oil.

3.1.4 Product Yields from Pyrolyzed Distillation Residues

The dry liquid organic yields from the pyrolysis of the distillation residues are shown in figure 3.5. The standard deviations for the yields were 1.2-2.0 wt. %. The ratios of the dry liquid organic yield reductions per wt. % bio-oil in reactor feed are shown in figure 3.6. The averaged ratios were 0.251 at 480°C and 0.395 at 500 °C. The standard deviations for the ratios were 0.043-0.103. The average pyrolyzed distillation ratios were 0.535 and 0.481 lower than the averaged ratios from the co-pyrolysis of ARC and raw bio-oil. This indicates the removal of the aqueous phase significantly increased the organic phase yields on a basis of bio-oil injected.

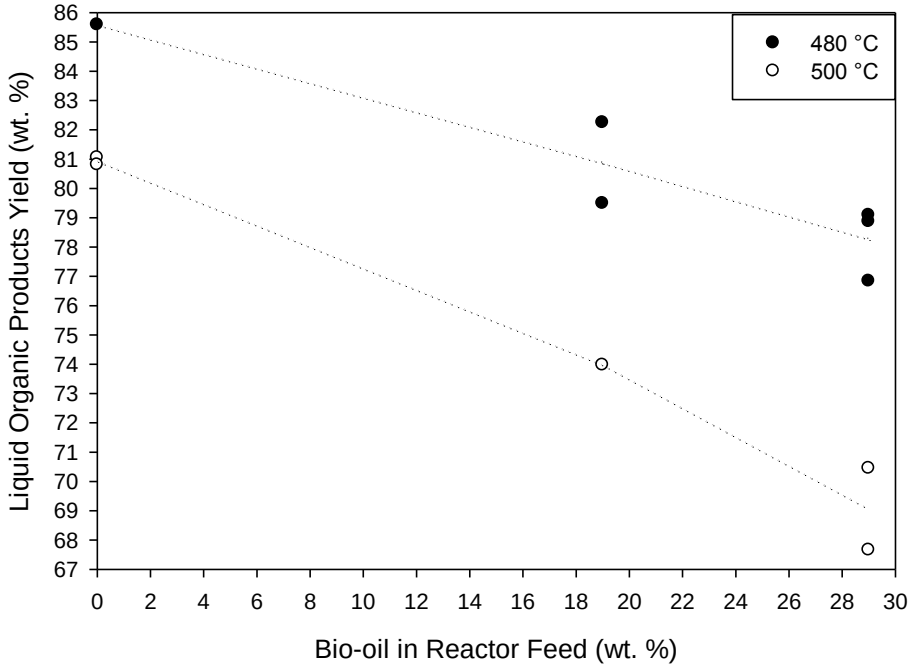

Figure 3.5 Dry Liquid Organic Product Yields from Pyrolyzed Distillation Residues

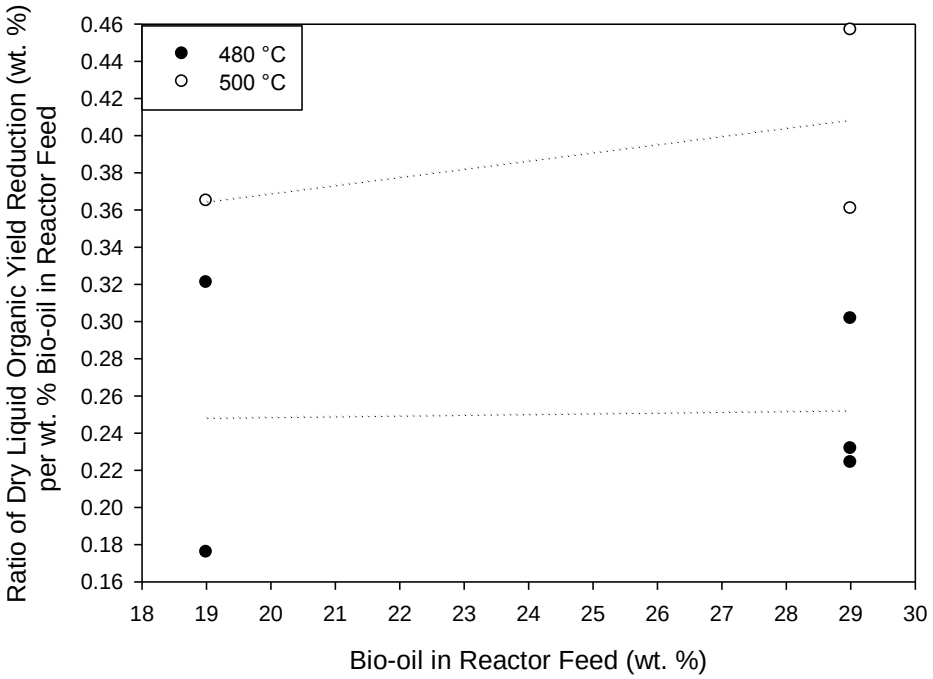

Figure 3.6 Liquid Organic Yield Reductions per wt. % Bio-oil in Reactor Feed Ratios

At 480 °C, the average ratios of dry liquid organic yield reductions per wt. % bio-oil in the reactor feed was identical for both of the distillation residues. This suggests there was a consistency to the distillation process described in section 2.3.1. Variances in liquid yields could have been caused by the inherent random nature of free radical thermal cracking of non-homogenous feedstocks, moisture analysis errors, and feedstock mixing issues. Some of the injected samples may have contained higher percentages of ARC molecules than other samples using the same distillation residue. Samples with higher percentages of ARC molecules would be expected to have higher liquid organics yields when compared to samples that contained higher percentages of bio-oil.

The water yields on a basis of approximated bio-oil injected from the pyrolysis of the distillation residues are shown in figure 3.7. The moisture analyses of 62.5 % of the liquid products indicated those products contained 0.5-2.0 wt. % water. The water yields on basis of approximated bio-oil injected for those experiments were 2.4-4.9 wt. %. The moisture analyses of the remaining 37.5 % liquid products indicated those products contained 3.6-4.5 wt. % water. The water yields on basis of approximated bio-oil injected for those experiments were 10.3-12.4 wt. %.

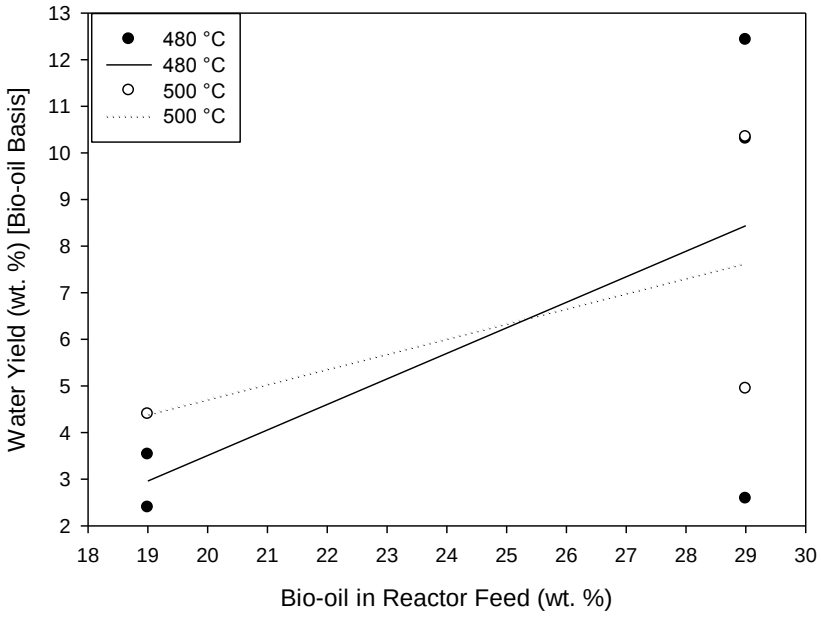

Figure 3.7 Bio-oil Basis Water Yields from Pyrolyzed Distillation Residues

As the liquid products were predominately composed of non-polar hydrocarbons, the polar water molecules remained in emulsions inside the hydrocarbons. The oxygen analyses of the liquid products suggest the Karl Fischer analyses overestimated the moisture contents of most of the organic phases. The increased water yields at the 29 wt. % mixing ratio were consistent with the heating value analysis described in section 3.6.2. Errors in moisture analyses would affect the liquid product distribution between liquid organic yields and water yields. The estimated potential variances in liquid product distribution due to moisture analysis errors were 1.2-2.7 wt. % on a basis of total mass injected. This could account for some of the variances in liquid yields.

The solid yields from the pyrolysis of the distillation residues are shown in figure 3.8. Experimental results with 6.6 wt. % and lower solid yields were considered outliers and omitted from figure 3.8. The standard deviations for the included solid yields were 0.6-1.8 wt. %. Half of the included solid yields were 0.8-1.2 wt. % higher than the pyrolysis of ARC at that temperature. The other half of the solid yields were either approximately equivalent or lower than the pyrolysis of ARC at the same temperature. The combination of the low number of experiments with the usage of a scale only accurate to ±0.5 g made the experimental data insufficient to prove whether the bio-oil in the reactor feed would increase or decrease relative to the pyrolysis of ARC.

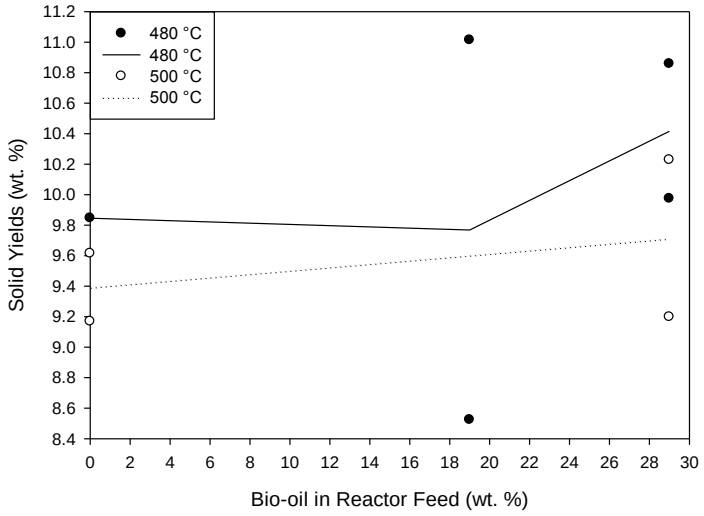

Figure 3.8 Solid Yields from Pyrolyzed Distillation Residues

The gas yields from the pyrolysis of the distillation residues are shown in figure 3.9. The gas yields were calculated by difference, so errors in solid or liquid yields would adversely affect the accuracy of the gas yields. The standard deviations for the gas yields were 0.03-1.6 wt. %. The ratios of gas yield increase per wt. % bio-oil in reactor feed are shown in figure 3.10. The standard deviations for the ratios were 0.002-0.06.

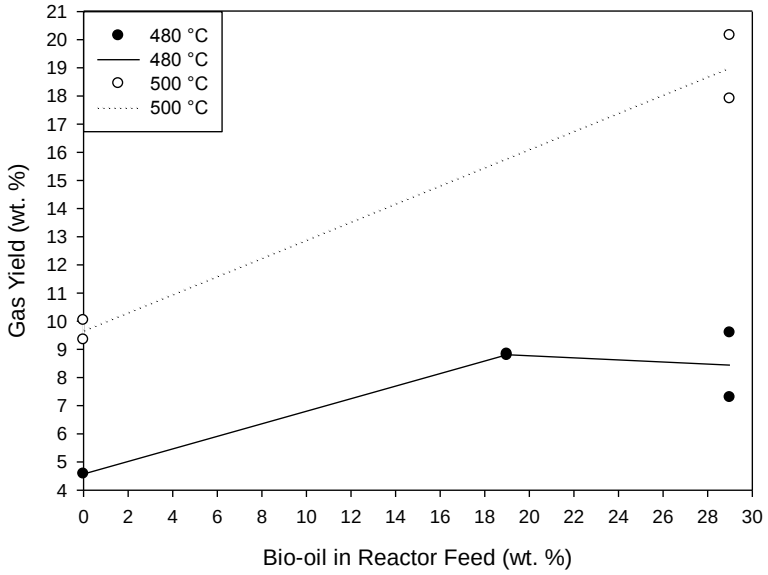

Figure 3.9 Gas Yields from Pyrolyzed Distillation Residues

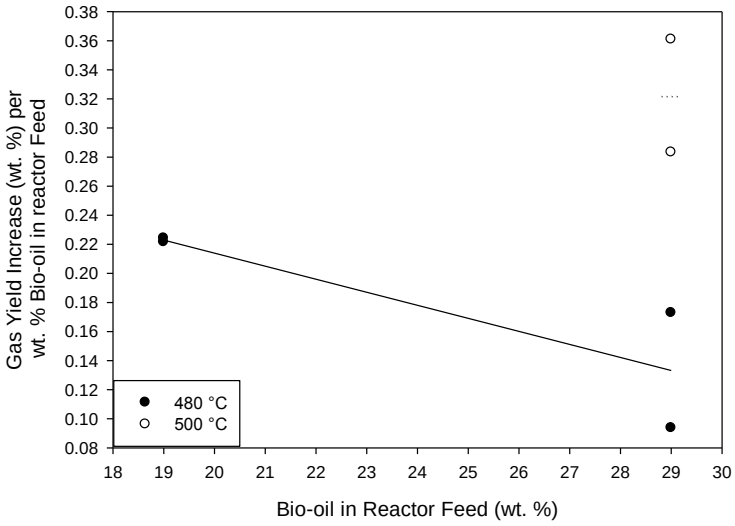

Figure 3.10 Ratios of Gas Yield Increases per wt. % Bio-oil in Reactor Feed

. The ratios of the wt. % difference in product yields per wt. % distilled bio-oil in the reactor feed were calculated for the liquid organics, water, solid, and gas yields for pyrolyzed distillation residues. The results at each mixing ratio and reactor temperature were averaged. The average ratios are shown in tables 3.1-3.2.

Table 3.1 Average Product Yield Δ per wt. % Distilled Bio-oil at 480 °C

Temperature: 480 °C	Average Δ Product Yield (wt. %)/wt. Bio-oil in Reactor Feed					
Feedstock	Liquid Organics	Water	Liquid Sum	Solid	Gas	Sum
Distilled Bio-oil (19)	-0.248	0.030	-0.218	-0.004	0.223	0.001
Distilled Bio-oil (29)	-0.252	0.084	-0.168	0.020	0.133	-0.015
Average Distilled	-0.251	0.062	-0.189	0.008	0.178	-0.003

Table 3.2 Average Product Yield Δ per wt. % Distilled Bio-oil at 500 °C

Temperature: 500 °C	Average Δ Product Yield (wt. %)/wt. Bio-oil in Reactor Feed					
Feedstock	Liquid Organics	Water	Liquid Sum	Solid	Gas	Sum
Distilled Bio-oil (19)	-0.366	0.044	-0.322			
Distilled Bio-oil (29)	-0.410	0.076	-0.334	0.011	0.322	-0.001
Average Bio-oil	-0.395	0.066	-0.329	0.011	0.322	0.004

The replacement of ARC with distilled bio-oil significantly reduced the liquid organics yields, while significantly increasing the gas yields and producing water. The temperature effects on the rate of secondary cracking reactions were higher for the distillation residues than it was for the ARC. Raising the freeboard temperature from 480 °C to 500 °C increased the 29 wt. % distillation residue average gas yield by 10.6 wt. %, but only raised the average gas yield of the ARC by 5.1 wt. %. The pyrolysis gas product studies of Sukiran et al. [72] have shown that hydrogen transfer to methoxy groups promotes methane production and can cause C-C bond rupture. Decarbonylation reactions would be expected to form CO [73]. Decarboxylation reactions would be expected to form CO_2 [73]. Carbonyl, carboxyl, and methoxyl functional groups are in some types phenolic compounds [74] that would have remained in the distillation residues.

After the bio-oil was distilled to remove the water and acids, the remaining platform chemicals as described in table 1.6 were phenolics, guaiacols, furfural, and Levoglucosan. These platform chemicals are all polar compounds that would be concentrated in the aqueous phase in the presence of a two phase mixture [75].

When ARC and raw bio-oil was co-pyrolyzed, the bio-oil contributed to the liquid products in the aqueous phase rather than the organic phase. When the aqueous phase was removed before pyrolysis, the bio-oil contributed to the liquid products in the organic phase. This observation should not be used as proof that the distillation process would allow bio-oil to be successfully integrated into a coker product stream. The bio-oil liquid products could have formed emulsions that would have to be broken up to prevent equipment corrosion and liquid product degradation. The addition of water to single phase bio-oils with low water contents to form two phase bio-oils have been studied by previous researchers [42, 76-78]. It is possible the liquid products of the bio-oil in the distillation residues would have migrated to an aqueous phase in a steam fluidized coker. It is also possible deoxygenation reactions during co-pyrolysis could have removed sufficient organic oxygen from the bio-oils to make them miscible in coker product streams. Demulsification and liquid product extraction experiments would need to be performed on the liquid products of the pyrolyzed distillation residues to determine more information about the feasibility of liquid product integration into coker product streams.

The pyrolysis water production from the pyrolysis of ARC and raw bio-oil was estimated by subtracting the estimated mass of water injected into the reactor from the mass of water in the liquid products. The estimated pyrolysis water yields during the co-pyrolysis of ARC and raw bio-oil were 43.7-58.4 wt. % of the estimated mass of injected organic bio-oil. When the aqueous phase was removed before co-pyrolysis, the estimated pyrolysis water yields were 2.4-12.4 wt. % of the estimated mass of injected bio-oil. This would be the equivalent of removing 71.6-95.9 wt. % of the water that would have been produced during co-pyrolysis in the distillation pre-treatment step, without using valuable hydrocarbons as hydrogen donors.

3.2.1 Co-pyrolyzed ARC and Bio-oil Liquid Product Moisture Analyses

The moisture analyses of the liquid products produced from the co-pyrolysis of ARC and raw bio-oil are shown in figures 3.11-3.12. The moisture analyses of the aqueous phases are shown in figure 3.11, and the moisture analyses of the organic phases are shown in figure 3.12.

When experimental data points in figures 3.11-3.12 are compared to each other, it seems likely that the moisture contents of the two phases were interrelated. Experiments with higher organic phase moisture contents were likely to have lower aqueous phase water contents and vice versa. This may have been dependent on the effectiveness of the mechanical separation of the phases. Samples that were more effectively separated would have organic phases with lower water contents than other samples. The aqueous phase moisture contents at 530 °C were 1.9-9.3 wt. % higher than the rest of the aqueous phases. The aqueous phase yields on a basis of injected bio-oil for the 530 °C experiments were 4.2-13.7 wt. % higher than the aqueous phase yields for the 480-500 °C experiments, as shown in figure 3.1. As the 530 °C experiments were performed after the 480-500 °C experiments, there is the possibility that the bio-oil feedstock had aged between the experiments. If this occurred, the injected mass of bio-oil at 530 °C would have had higher moisture contents than the injected bio-oil at 480-500 °C [42].

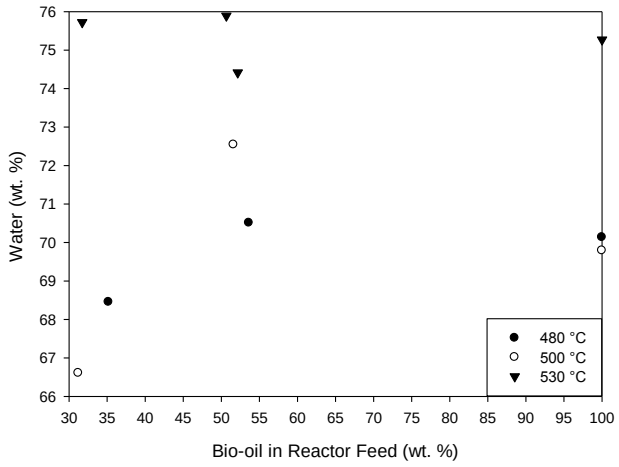

Figure 3.11 Co-pyrolyzed ARC and Bio-oil Aqueous Phase Moisture Contents

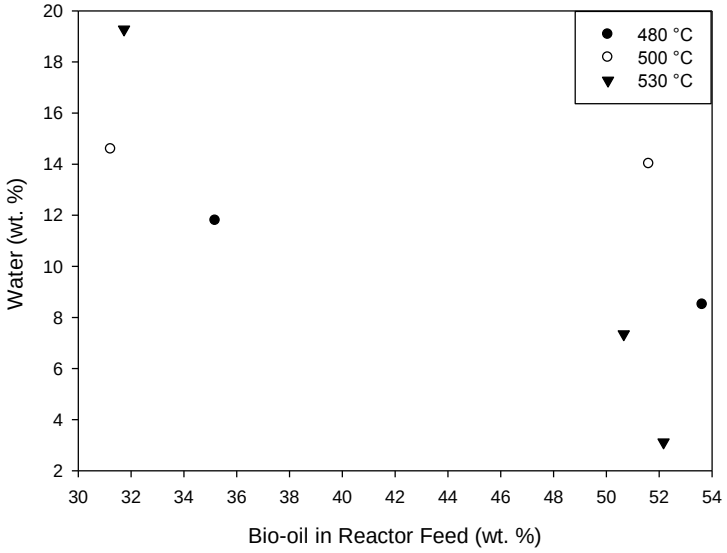

Figure 3.12 Co-pyrolyzed ARC and Bio-oil Organic Phase Moisture Contents

3.2.2 Pyrolyzed Distillation Residue Liquid Product Moisture Analyses

The moisture analyses of the liquid products produced from the pyrolyzed distillation residues are shown in figure 3.13. The standard deviations were 0.2-1.8 wt. %.

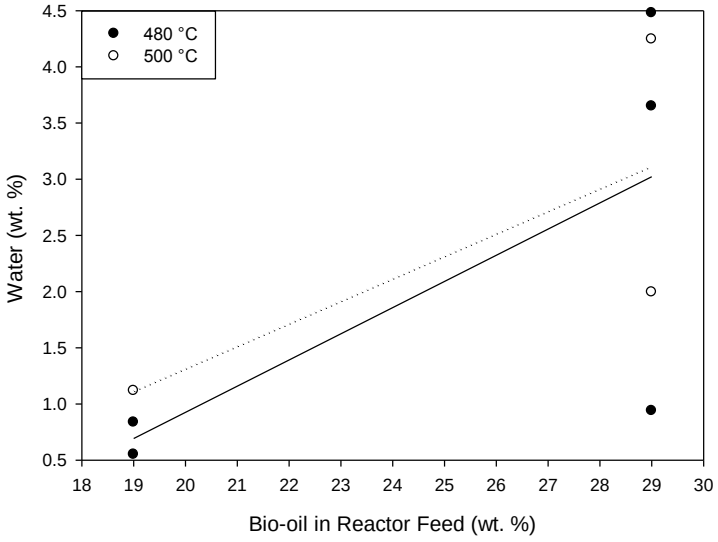

Figure 3.13 Pyrolyzed Distillation Residue Liquid Product Moisture Contents

3.3.1 Co-pyrolyzed ARC and Bio-oil Liquid Product Elemental Analyses

The elemental analyses of the liquid phases produced through the co-pyrolysis of ARC with raw bio-oil were converted to a dry basis using equations 2.1-2.3.

The aqueous phase results are shown in figures 3.14-3.16. Two of the hydrogen contents were omitted as the organic hydrogen contents were calculated to have negative weight percentages. As the moisture contents of those two samples were not higher than the rest of the aqueous samples, it is more likely the errors were caused by experimental error in the measurement of the elemental analyses. Comparing the samples on a wet basis did not remove the variability in elemental compositions between similar samples. The co-pyrolyzed aqueous phases typically had higher organic hydrogen contents than the pyrolysis of raw bio-oil. This is consistent with the expected result of the water formation reactions promoting organic hydrogen deficiencies without the addition of ARC hydrogen donors. The aqueous phases at 530 °C had increased carbon contents and lower organic oxygen contents at 530 °C when compared to aqueous phases at 480-500 °C. This was caused by the increase in moisture content relative to the samples at 480-500 °C.

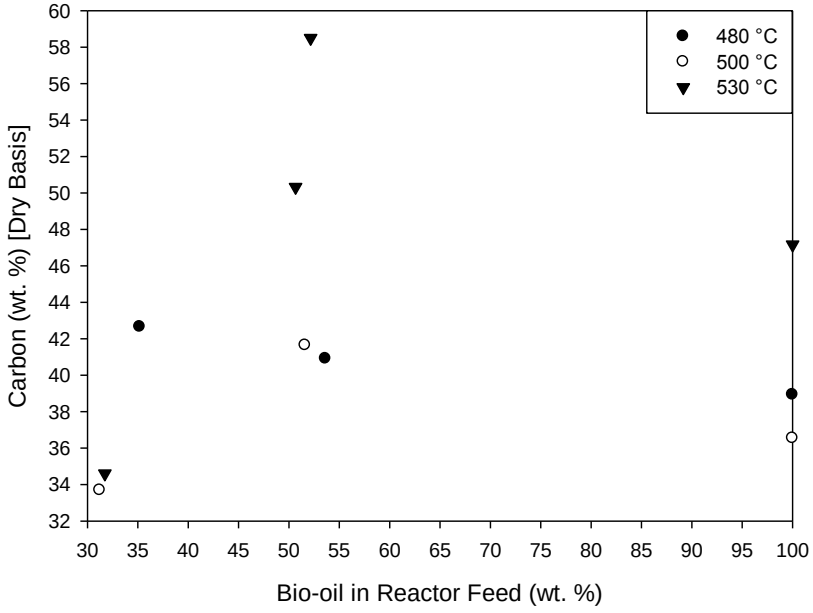

Figure 3.14 Co-pyrolyzed ARC and Bio-oil Aqueous Phase Carbon Content

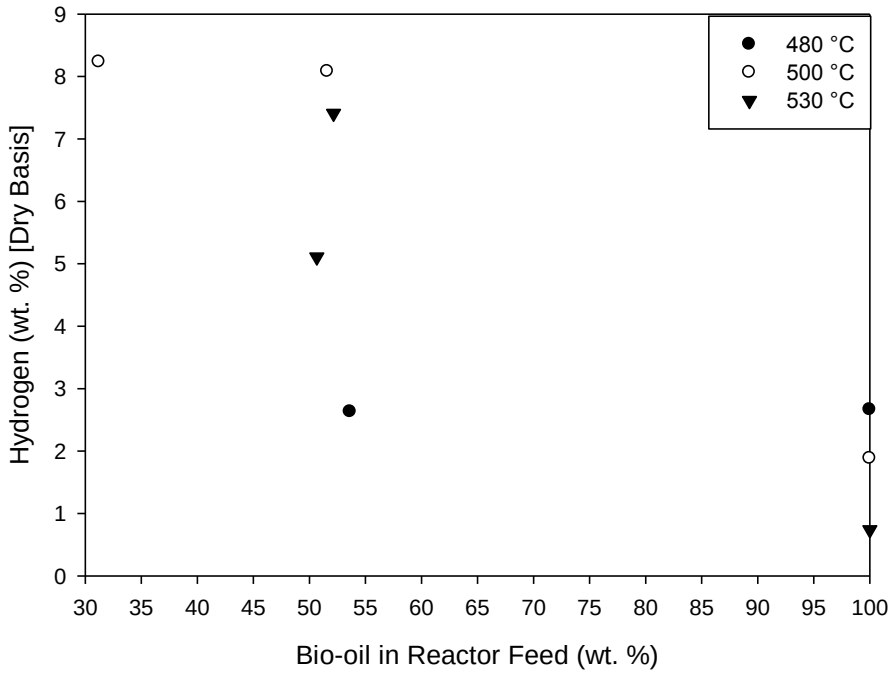

Figure 3.15 Co-pyrolyzed ARC and Bio-oil Aqueous Phase Hydrogen Content

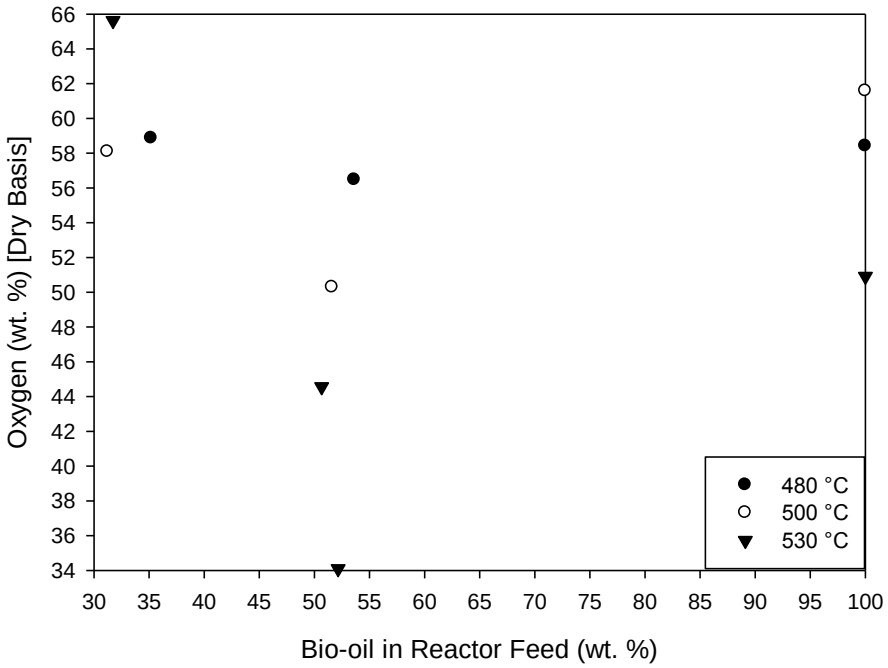

Figure 3.16 Co-pyrolyzed ARC and Bio-oil Aqueous Phase Oxygen Content

The dry basis organic oxygen contents of the organic phases were consistently calculated to be negative with the exception of the sample with a moisture content of 3.1 wt. %. That sample was shown to have a dry basis oxygen content of 1.0 wt. %. This indicates either the oxygen elemental analyses of the organic phases were significantly underestimated by the elemental analyzer, or the moisture analyses were overestimated by the KF titrator. As the sum of the carbon, hydrogen, oxygen, sulfur, and nitrogen contents fell in the ranges of 97.0-104.0 wt. %, this indicates that the moisture analyses of the organic phases were probably overestimated by the Karl Fischer titrator.

The wet basis elemental analyses of the organic phases of the co-pyrolysis of ARC and bio-oil are shown in figures A.1-A.4. The oxygen contents of the co-pyrolyzed samples were consistently in the range of 3.5-4.5 wt. % for both mixing ratios, which were 0.3-1.3 wt. % higher than the oxygen content of the liquid products of the pyrolysis of ARC. The experimental data was insufficient to find any correlations based off of the reactor temperature or the mixing ratio for the carbon, hydrogen, or sulfur contents. Similarly the experimental data was insufficient to find any correlations based off of the reactor temperature or the mixing ratio for the H/C ratios of the organic phases.

3.3.2 Pyrolyzed Distillation Residue Liquid Product Elemental Analyses

The wet basis elemental analyses of the liquid products of the pyrolyzed distillation residues are shown in figures 3.17-3.20. The standard deviations for the carbon contents were 0.4-1.7 wt. %. The standard deviations for the hydrogen contents were 0.01-0.08 wt. %. The standard deviations for the sulfur contents were 0.1-0.5 wt. %. The standard deviations for the oxygen contents were 0.07-0.7 wt. %.

The ratios of the wt. % difference in liquid product element content per wt. % distilled bio-oil in the reactor feed were calculated for the carbon, hydrogen, oxygen, sulfur, and nitrogen contents for pyrolyzed distillation residues. The results at each mixing ratio and reactor temperature were averaged. The average ratios are shown in tables 3.3-3.4.

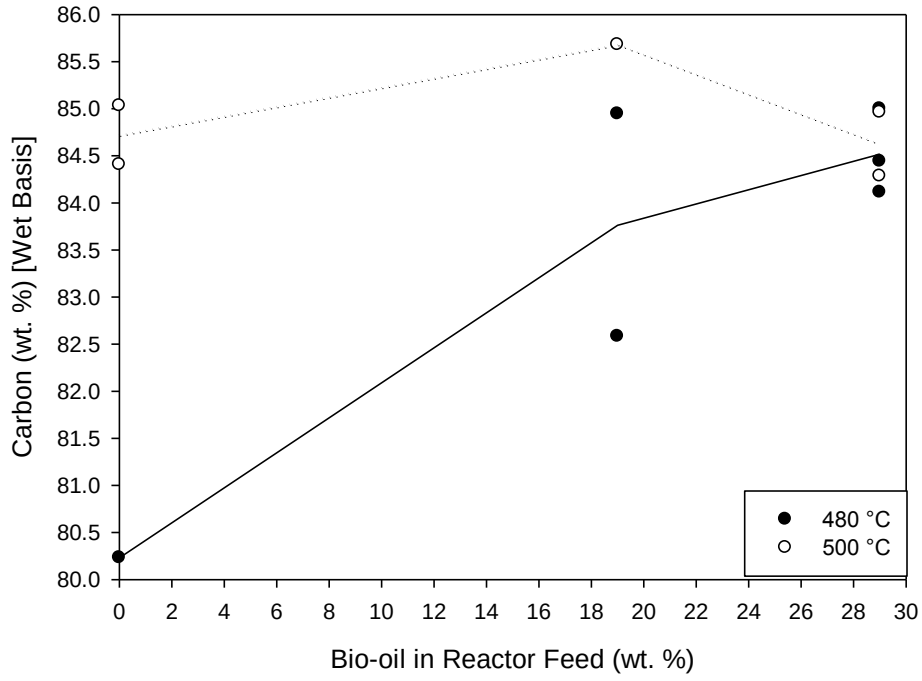

Figure 3.17 Pyrolyzed Distillation Residue Liquid Product Carbon Content

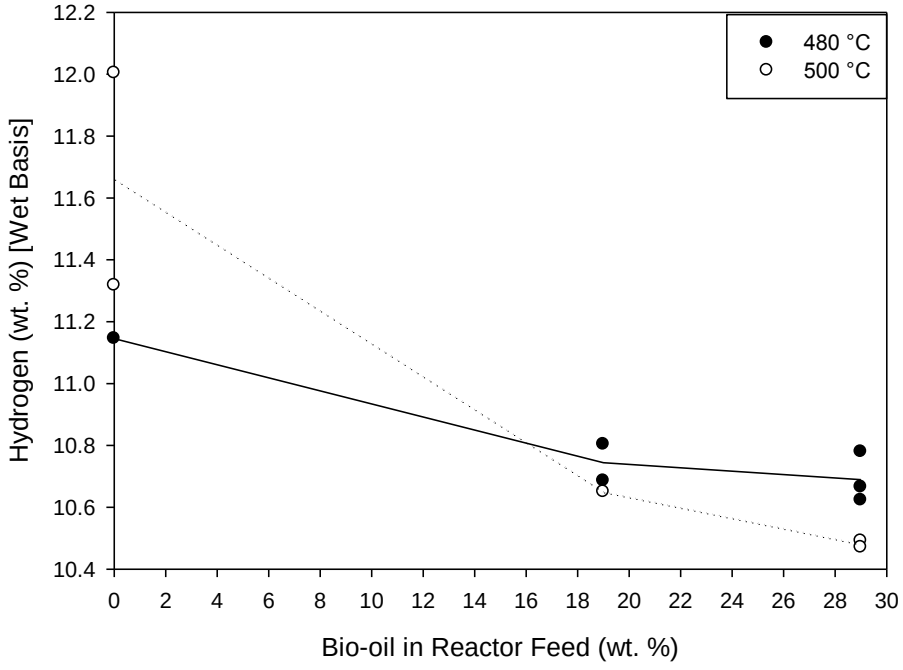

Figure 3.18 Pyrolyzed Distillation Residue Liquid Product Hydrogen Content

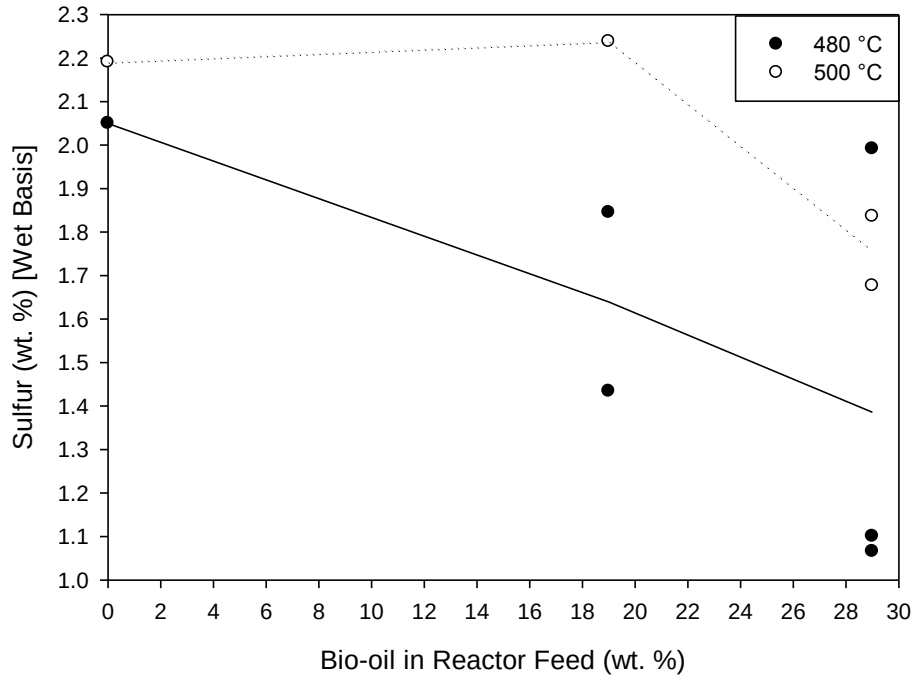

Figure 3.19 Pyrolyzed Distillation Residue Liquid Product Sulfur Content

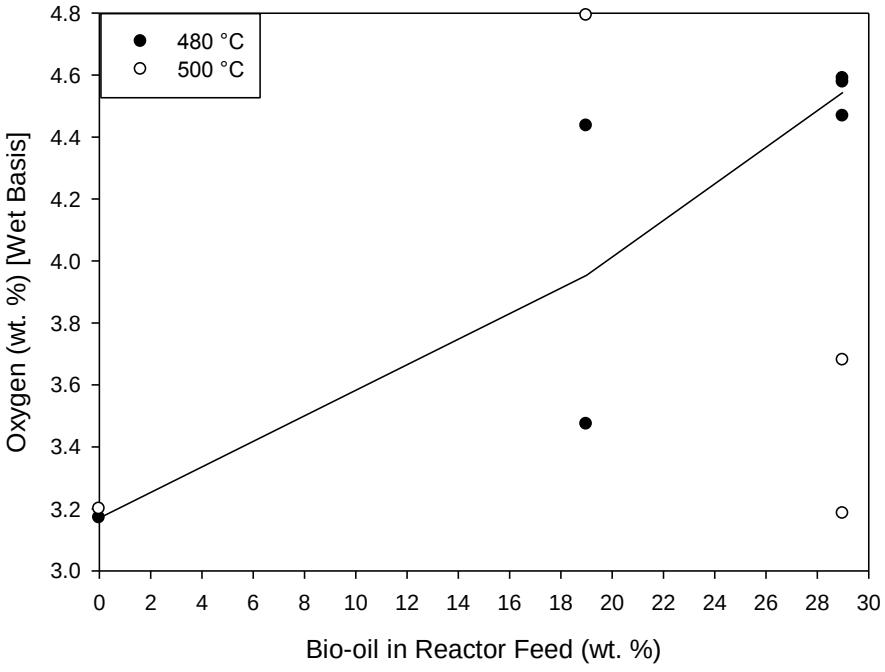

Figure 3.20 Pyrolyzed Distillation Residue Liquid Product Oxygen Content

Table 3.3 Average Liquid Product Elemental Content Δ per wt. % Bio-oil at 480 °C

Temperature: 480 °C	Average Δ Elemental Content (wt. %)/wt. Bio-oil in Reactor Feed					
Feedstock	Carbon	Hydrogen	Oxygen	Sulfur	Nitrogen	Sum
Distilled Bio-oil (19)	0.1859	-0.0211	0.0412	-0.0216	0.0069	0.1913
Distilled Bio-oil (29)	0.1478	-0.0157	0.0474	-0.0229	0.0014	0.1580
Average Distilled	0.1631	-0.0179	0.0449	-0.0224	0.0036	0.1713

Table 3.4 Average Liquid Product Elemental Content Δ per wt. % Bio-oil at 500 °C

Temperature: 500 °C	Average Δ Elemental Content (wt. %)/wt. Bio-oil in Reactor Feed					
Feedstock	Carbon	Hydrogen	Oxygen	Sulfur	Nitrogen	Sum
Distilled Bio-oil (19)	0.0506	-0.0532	0.0838	0.0025	0.0071	0.0908
Distilled Bio-oil (29)	-0.0033	-0.0407	0.0080	-0.0150	-0.0014	-0.0524
Average Distilled	0.0147	-0.0449	0.0333	-0.0092	0.0015	-0.0046

When compared to the liquid products of the pyrolysis of ARC, the oxygen contents of the liquid products increased, while the hydrogen and sulfur contents of the liquid products decreased. When compared to the liquid products of the pyrolysis of ARC, the carbon contents of the liquid products increased with the exception of the 29 wt. % experiments at 500 °C. There was no significant change in liquid product carbon contents of the pyrolysis of the 29 wt. % distillation residue at 500 °C relative to the liquid products of ARC. The large carbon content increases in the co-pyrolysis liquid products relative to the pyrolysis of ARC at 480 °C is erroneous due to the unrealistically low carbon content observed from the liquid products of the pyrolysis of ARC at 480 °C. The 80.2 wt. % carbon content would likely become an outlier with larger sample sizes.

The atomic H/C ratios of the liquid products of the pyrolyzed distillation residues are shown in figure 3.21. The H/C ratios were 1.49-1.54 at 480 °C, and 1.47-1.48 at 500 °C. The standard deviations were 0.01-0.02. The H/C ratios of the pyrolyzed distillation residue liquid products were similar to the 1.51 H/C ratio of No. 6 fuel oil [79]. To put things in perspective, common targets for H/C ratios are 2.0 (diesel) [80] and 2.1 (gasoline) [79].

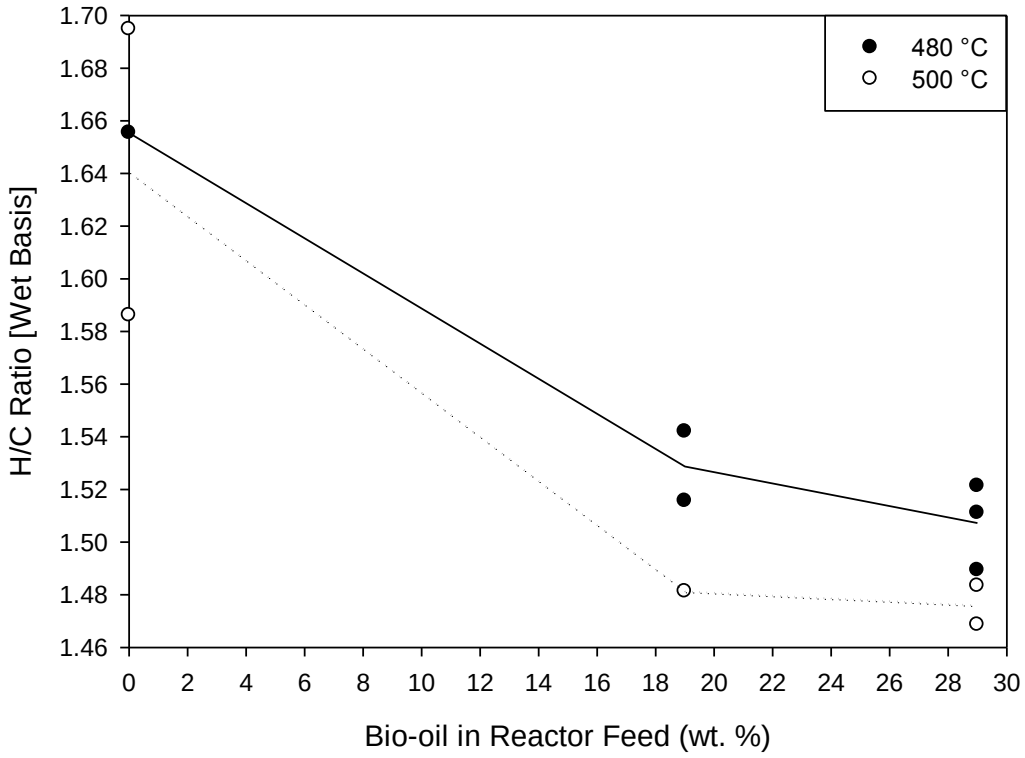

Figure 3.21 Liquid Product H/C Ratios from Pyrolyzed Distillation Residues

The H/C reductions in the pyrolyzed distillation residues were a result of the increase in gas production caused by the replacement of ARC in the reactor feed with bio-oil. As shown in figures A.5-A.6, 61.1-68.3 mol. % of the atoms in the pyrolyzed distillation residue gas were hydrogen atoms. The gas products (described in section 3.5.2) were predominately composed of alkanes with high H/C ratios. An increase in production of alkane gases would therefore reduce the H/C ratio of the liquid products.

The reductions in the H/C ratios of the liquid products were consistent with the changes in gas yields as shown in figure 3.9. When the freeboard temperature was raised from 480 °C to 500 °C, the gas yields increased by 8.3-12.8 wt. %, and the H/C ratios were reduced by 0.006-0.06. At 480 °C, there was only a 0.4 wt. % difference in average gas yields of the two pyrolyzed distillation residues. There was only a 0.02 difference in average H/C ratios for the liquid products of the two distillation residues at 480 °C.

3.4.1 Co-pyrolyzed ARC and Bio-oil Gas Product Composition

The compositions of the pyrolysis gas produced from the co-pyrolysis of ARC and raw bio-oil are shown in figures 3.22-3.23. The pyrolysis of ARC produced pyrolysis gases containing 0.9-2.4 wt. % CO, 0.2-1.1 wt. % CO_2, and 97.3-98.8 wt. % alkanes/alkenes. The reactor temperature did not have any significant effects on the pyrolysis gas produced from the pyrolysis of ARC. At 530 °C, the pyrolysis of bio-oil produced pyrolysis gas containing 58.5 wt. % CO, 22.0 wt. % CO_2, and 19.5 wt. % alkanes/alkenes. At 530 °C, the average gas composition of the pyrolysis gases from the co-pyrolysis of ARC and bio-oil at the ~51 wt. % mixing ratio were 29.3 wt. % CO, 7.3 wt. % CO_2, and 63.3 wt. % alkanes/alkenes. The replacement of ARC in the reactor feed increased the CO and CO_2 contents of the gas products, while reducing the alkane and alkene contents of the gas phase.

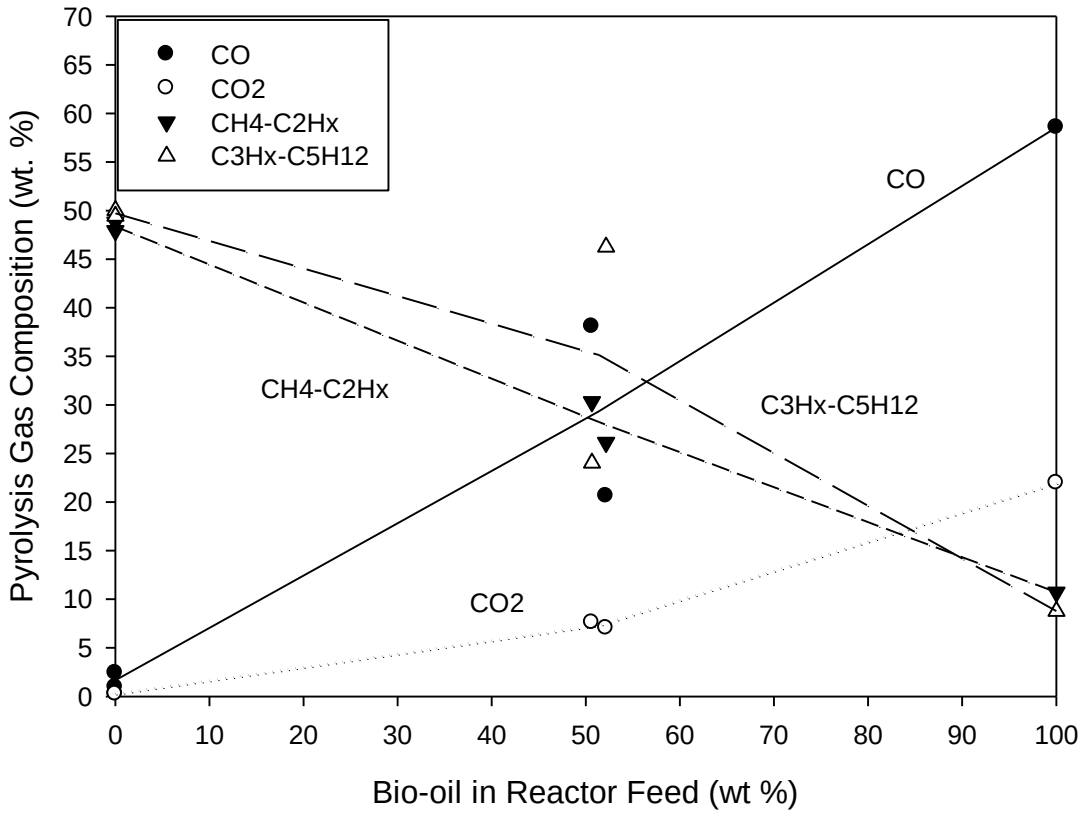

Figure 3.22 Co-pyrolyzed ARC and Raw Bio-oil Gas Compositions at 530 °C

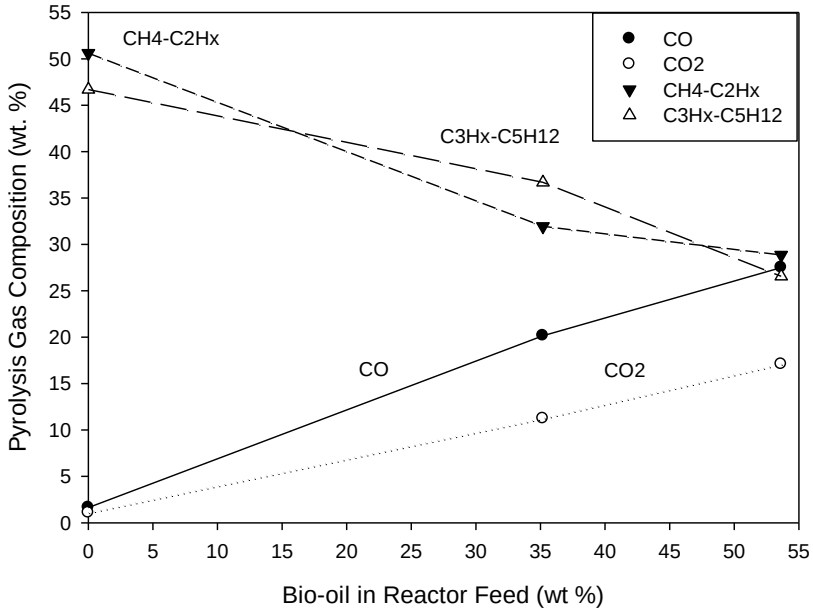

Figure 3.23 Co-pyrolyzed ARC and Raw Bio-oil Gas Compositions at 480 °C

3.4.2 Pyrolyzed Distillation Residue Gas Product Composition

The compositions of the gas produced from the pyrolysis of the distillation residues are shown in figures 3.24-3.25. The replacement of ARC in the reactor feed with distilled bio-oil reduced the alkane/alkene content of the pyrolysis gas, while increasing the CO and CO_2 contents. There were no observable trends or correlations to any changes to the gas composition based off the reactor temperature.

The effect of the bio-oil aqueous phase on the pyrolysis gas composition at 480 °C can be determined by comparing the data in figures 3.23-3.24. The distilled pyrolysis gases at 480 °C contained on average 6.8-7.9 wt. % lower CO_2 contents and higher alkane/alkene contents than the equivalent dry basis mixing ratio experiments co-pyrolyzing ARC and raw bio-oil. The removal of the aqueous phase before pyrolysis removed the carboxylic acids with boiling points lower than 130°C from the bio-oil. The pyrolysis of carboxyl groups forms CO_2 by decarboxylation [81], so the removal of carboxylic acids lowered the CO_2 production relative to the pyrolysis of raw bio-oil.

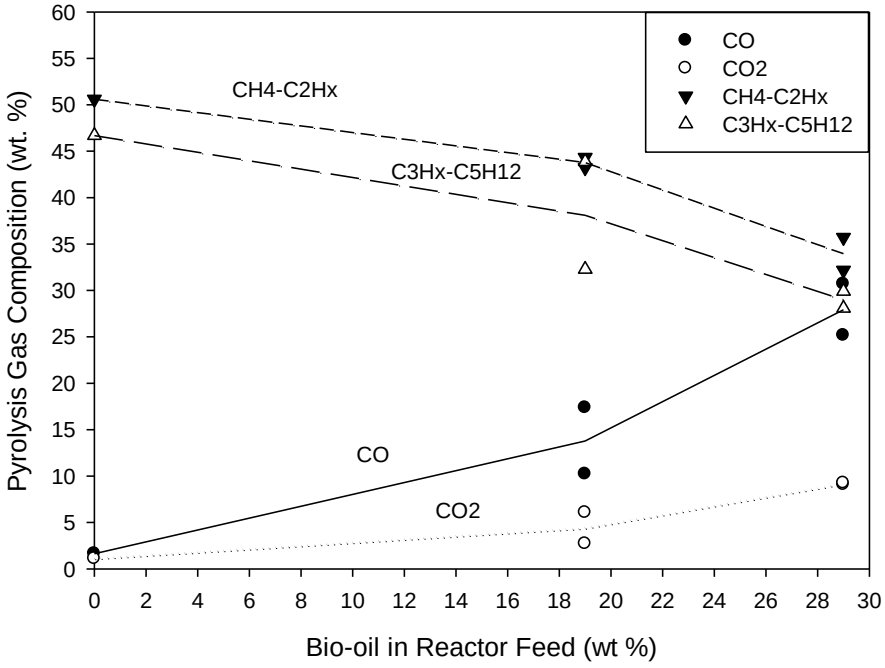

Figure 3.24 Pyrolyzed Distillation Residue Gas Compositions at 480 °C

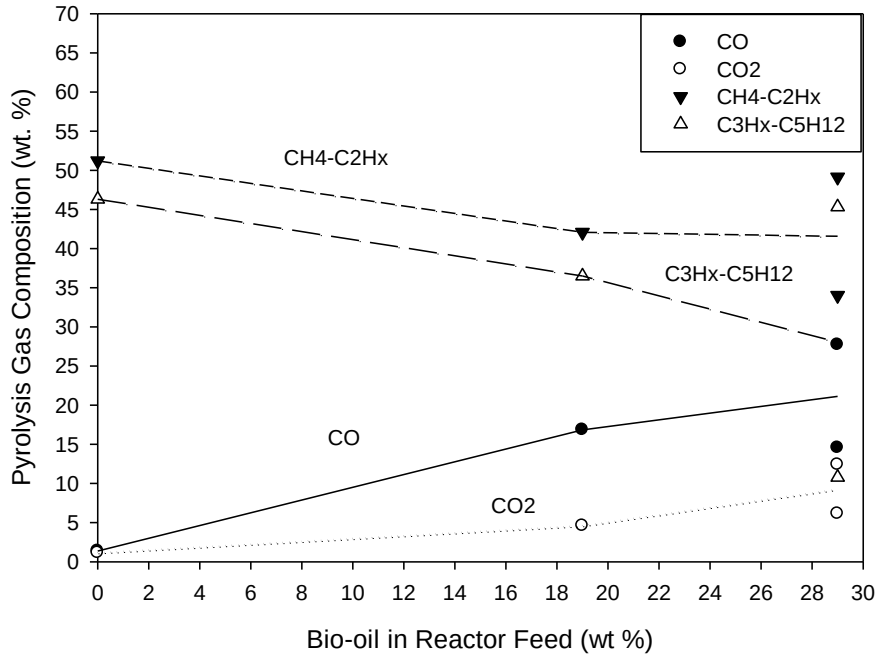

Figure 3.25 Pyrolyzed Distillation Residue Gas Compositions at 500 °C

3.5.1 Co-pyrolyzed ARC and Bio-oil Organic Phase High Heating Values

The high heating values (HHVs) of the organic phases produced from the co-pyrolysis of ARC and raw bio-oil are shown in figure A.7. The pyrolysis of ARC produced liquid products with 41.4-43.4 kJ/g HHVs. The co-pyrolysis of ARC and bio-oil produced organic phases with 32.7-42.0 kJ/g HHVs. When the reactor temperature was increased, the heating values of the organic phases usually decreased. This was likely caused by the increased rate of secondary cracking reactions relative to the lower reactor temperatures, which reduced the H/C ratios as discussed in section 3.4.2.

The organic phases produced at the lower mixing ratios had lower high heating values than the organic phases produced at the higher mixing ratios. This was due to inconsistencies of the mechanical separation of the two phases which caused the organic phases at the lower mixing ratios to have higher moisture contents as shown in figure 3.12. As the presence of water reduces the high heating values relative to dry fuels [82], the organic phases with higher moisture contents would be expected to have lower HHVs. The dry basis high heating values as shown in figure A.8 may have been overstated due to the probable overestimation of the moisture contents by the Karl Fischer titrator as described in section 3.4.1.

3.5.2 Pyrolyzed Distillation Residue Liquid Product High Heating Values

The high heating values of the liquid products produced from the pyrolysis of the distillation residues are shown in figure 3.26. The pyrolysis of the distillation residues produced liquid products with 38.0-42.5 HHVs. The standard deviations were 0.8-2.5 kJ/g. The replacement of ARC with distilled bio-oil reduced the heating values of the liquid products relative to the pyrolysis of ARC. The large standard deviations in heating values were consistent with the large deviations in moisture contents as shown in figure 3.13. Calculating the high heating values on a dry basis did not remove the variations in heating values as shown in figure A.9.

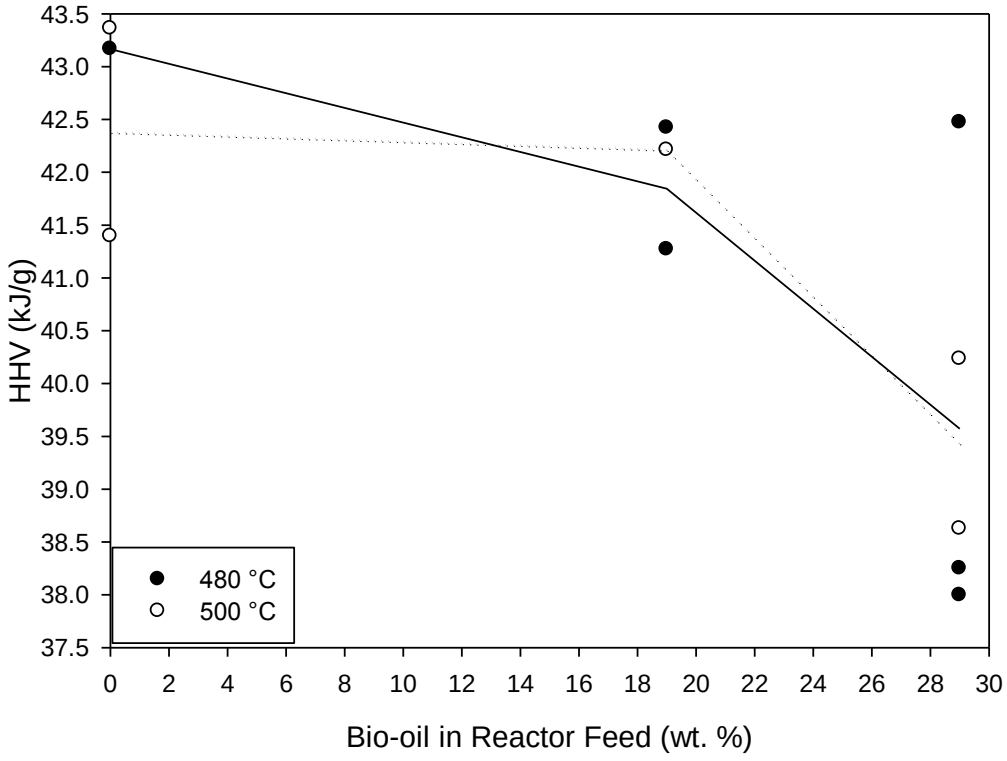

Figure 3.26 Pyrolyzed Distillation Residues Liquid Product High Heating Values

The high heating values of the integrated bio-oil were approximated by assuming the ARC contributions to the liquid product masses and released energy from combustion would be identical to the pyrolysis of ARC at that temperature. The remaining liquid product masses and released energy from combustion were attributed to the bio-oil.

The approximated high heating values for the estimated mass of integrated bio-oil are shown in figure A.10. The average approximated high heating values for the integrated bio-oil were 29.4 kJ/g at 480 °C and 29.7 kJ/g at 500 °C. The standard deviations were 9.6 kJ/g at 480 °C and 11.7 kJ/g at 500 °C. As a comparison, the distilled bio-oil studied by Zheng et al. [55] had a lower heating value (LHV) of 34.2 kJ/g. The approximated high heating value of the integrated bio-oil was significantly higher than the 17.4 kJ/g HHV of the raw bio-oil (table 2.1), but still significantly less than the ~42-43 kJ/g HHVs required for integration into diesel or gasoline product streams [83].

3.6.1 Pyrolyzed Distillation Residue Liquid Product Densities and Viscosities

The densities of the liquid products from pyrolyzed distillation residues are shown in figure 3.27. The pyrolysis of ARC produced liquid products with densities of 0.926 g/cm^3 at 480 °C and 0.933 g/cm^3 at 500 °C. The pyrolyzed 19 wt. % distillation residues produced liquid products with densities of 0.935-0.936 g/cm^3 at 480 °C and 0.942 g/cm^3 at 500 °C. The pyrolyzed 29 wt. % distillation residues produced liquid products with densities of 0.931-0.962 g/cm^3 at 480 °C and 0.933-0.936 g/cm^3 at 500 °C. The standard deviations for the 29 wt. % liquid product densities were 0.002-0.016 g/cm^3.

The dynamic viscosities of the liquid products from pyrolyzed distillation residues are shown in figure 3.28. The pyrolysis of ARC produced liquid products with viscosities of 18.2 cP at 480 °C and 13.1 cP at 500 °C. The pyrolyzed 19 wt. % distillation residues produced liquid products with viscosities of 19.0 cP at 480 °C and 20.8 cP at 500 °C. The pyrolyzed 29 wt. % distillation residues produced liquid products with viscosities of 16.4-22.4 cP at 480 °C and 11.4-11.6 cP at 500 °C. The standard deviations for the 29 wt. % liquid product viscosities were 0.1-3 cP.

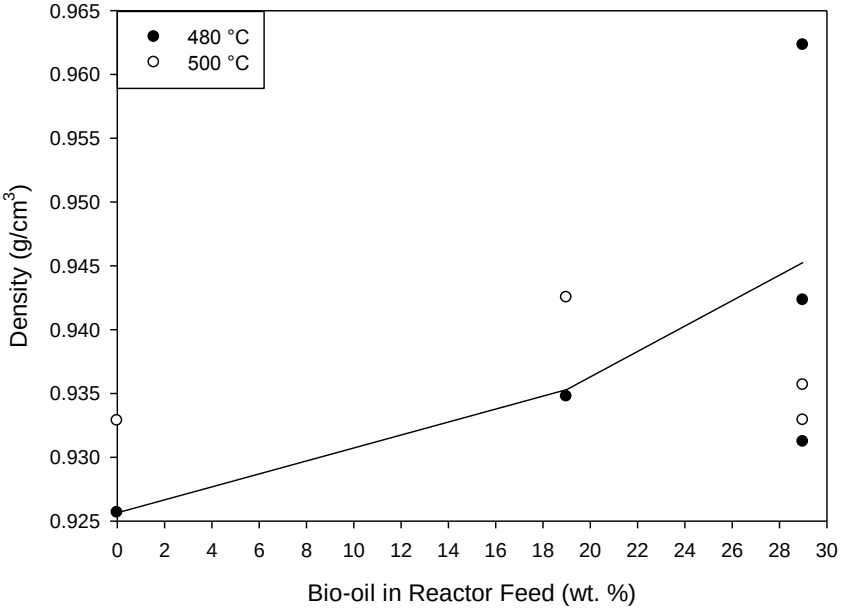

Figure 3.27 Liquid Product Densities from Pyrolyzed Distillation Residues

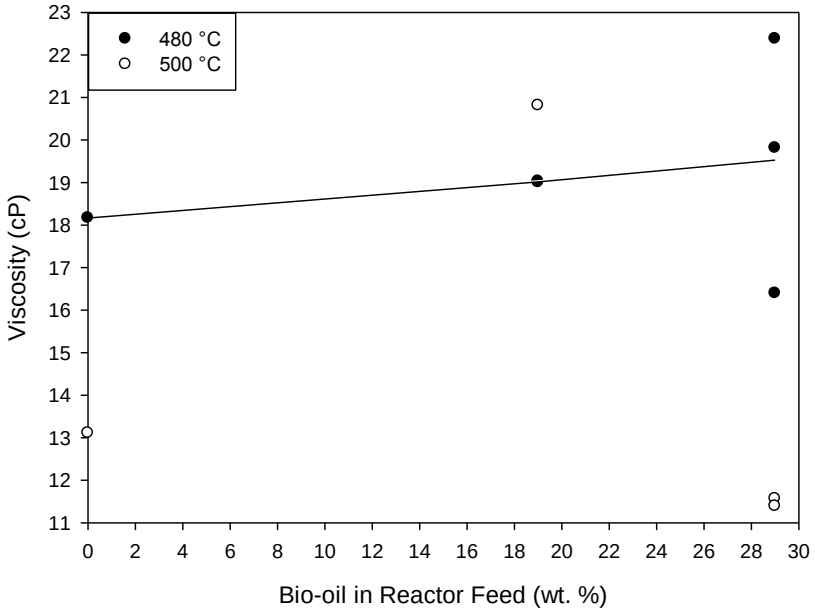

Figure 3.28 Liquid Product Viscosities from Pyrolyzed Distillation Residues

At 480 °C, the averaged densities and averaged viscosities of the liquid products increased relative to the liquid products of ARC with increasing proportions of distilled bio-oil in the reactor feed. At 500 °C, the densities and viscosities of the liquid products of the 19 wt. % distillation residue increased relative to the liquid products of ARC. At 500 °C, the densities of the liquid products of the 29 wt. % distillation residue were approximately the same as the liquid products of the pyrolysis of ARC. At 500 °C, the viscosities of the liquid products of the 29 wt. % distillation residue were 1.5-1.7 cP lower than the liquid products of the pyrolysis of ARC.

At 500°C there is a similar pattern to the liquid product densities (figure 3.27), viscosities (figure 3.28), and the liquid product oxygen content (figure 3.20). The liquid product oxygen contents, densities, and viscosities all increased with increasing proportions of distilled bio-oil at 480 °C. The densities and viscosities of bio-oil are higher than those of petroleum based transportation fuels such as gasoline and diesel [84]. The densities and viscosities of bio-oil have been shown to decrease as the water content of the bio-oil increases [42]. The viscosities and densities of the liquid products of the

pyrolysis of the 19 wt. % distillation residue may have been disproportionately higher due to disproportionate organic oxygen content relative to the water oxygen content when compared to the 29 wt. % liquid products which had higher moisture contents.

Chapter 4: Conclusions

Atmospheric reduced crude (ARC) and raw birchwood bio-oil was simultaneously pyrolyzed in a mechanically fluidized reactor (MFR). The condensed liquid products formed a two-phase mixture consisting of an aqueous phase and an organic phase. The organic phase yields indicated there was very little integration of bio-oil molecules into the organic phase. The condensed bio-oil molecules were concentrated in the aqueous phase. The co-pyrolysis promoted water formation relative to the pyrolysis of bio-oil, which indicates some of the ARC molecules acted as hydrogen donors during co-pyrolysis.

The integration of raw bio-oil into a Fluid Coker^{TM} would not be advisable. The liquid products of the bio-oil were not miscible with existing petroleum refinery product streams. The integration of bio-oil into an existing refinery would require the installation of an entirely separate liquid processing system to process the aqueous products from the bio-oil. The quality of the coker gas oil produced through co-processing would also have been reduced due to lower heating values caused by the loss of hydrogen during water formation with organic bio-oil molecules.

Raw bio-oil was capable of being distilled without any noticeable polymerization to 130 °C when diluted with atmospheric reduced crude (ARC) in a well mixed vessel. The distillation successfully removed the aqueous products of bio-oil from the coking process in order to be more compatible with refinery infrastructure which does not extract valuable aqueous products from water waste streams. There was no evidence of coking in the bio-oil. The integrated organic bio-oil in the resulting distillation residues seemed to be initially miscible in the ARC. The consistency of the distillation residues changed after several weeks. It is not known if the consistency changes would have occurred at room or refrigerated temperatures. The feedstocks were repeatedly heated before each experiment, so the consistency changes may or may not have been caused or accelerated by thermal degradation. It is possible the consistency changes would have occurred at room temperature or refrigerated temperatures.

The pyrolysis of the distillation residues produced one phase liquid products with only 0.5-4.5 wt. % water. Unlike the pyrolysis of ARC and untreated bio-oil which produced very fine solids that provided significant contaminated the liquid products and possibly catalyzed water formation, the liquid products from the pyrolysis of the distillation residues contained no detectable solids. It was not known if the addition of water to the liquid products would promote phase separation into a two-phase mixture.

The liquid products of the pyrolyzed distillation residues contained 3.2-4.8 wt. % oxygen. The oxygen content of the liquid products was too high to be processed in a catalytic cracker without being treated in a hydrotreater, but significantly lower than the 51.4 wt. % (dry basis) oxygen content of pure untreated bio-oil. The estimated high heating values of the integrated bio-oil were 29.4-29.7 kJ/g. The high heating values of the integrated bio-oil were significantly higher than the 17.4 kJ/g high heating values of the raw bio-oil, but significantly less than the 42-43 kJ/g high heating values of coker gas oils. The integrated distilled bio-oil increased the densities and viscosities of the liquid products relative to the liquid products of the pyrolysis of ARC. As the increases in density and viscosity seem to be caused by the organic oxygen content of the integrated bio-oil, hydrotreating the integrated bio-oil may reduce the liquid densities and viscosities to typical coker gas oil levels.

The replacement of ARC in the reactor feed with distilled bio-oil significantly increased the gas yields and produced on average 6.2-6.6 wt. %/wt. % distilled bio-oil in the reactor feed. The increases in gas yields may have been predominately caused by decarbonylation of carbonyl groups, decarboxylation of carboxyl groups, and hydrogen transfer to methoxyl groups. It might be possible to promote the water formation and removal of the carbonyl, carboxyl, and methoxyl groups during the hydrotreatment of the distilled bio-oil.

Chapter 5: Recommendations for Future Work

- Perform thorough experiments to determine which fractions of bio-oil would optimally processed in a bio-refinery to recover valuable aqueous products, and which fractions would optimally be processed in a petroleum refinery to produce transportation fuels
- Investigate the multi-stage process of bio-oil distillation (vacuum distillation or co-distillation with petroleum feedstocks)→hydrotreat the distillation residues →co-process the hydrotreated distillation residues with vacuum reduced crude in Fluid Cokers^{TM} and delayed cokers.
- Analyze the liquid products at each step of the process using a GC-MS-FID column and method optimized for the identification and quantification of petroleum products.
- Analyze the liquid products at each step to determine the elemental analyses, heating values, densities, and viscosities of the liquid products.
- Perform stability determining experiments on different temperature cuts of bio-oils produced through fractional condensation to determine what temperatures the fractions can be heated without degradation.
- If it is determined that some of the bio-oil fractions produced through fractional condensation can be heated to 375 °C without decomposition, perform experiments injecting those fractions into a crude distillation unit typically used in the petroleum industry.

Appendix

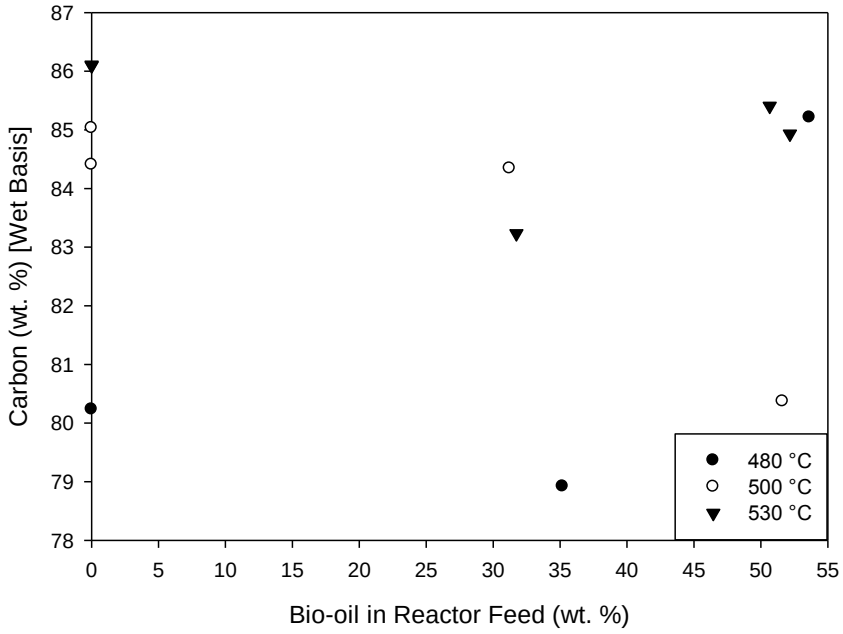

Figure A.1 Co-pyrolyzed ARC and Bio-oil Organic Phase Carbon Content

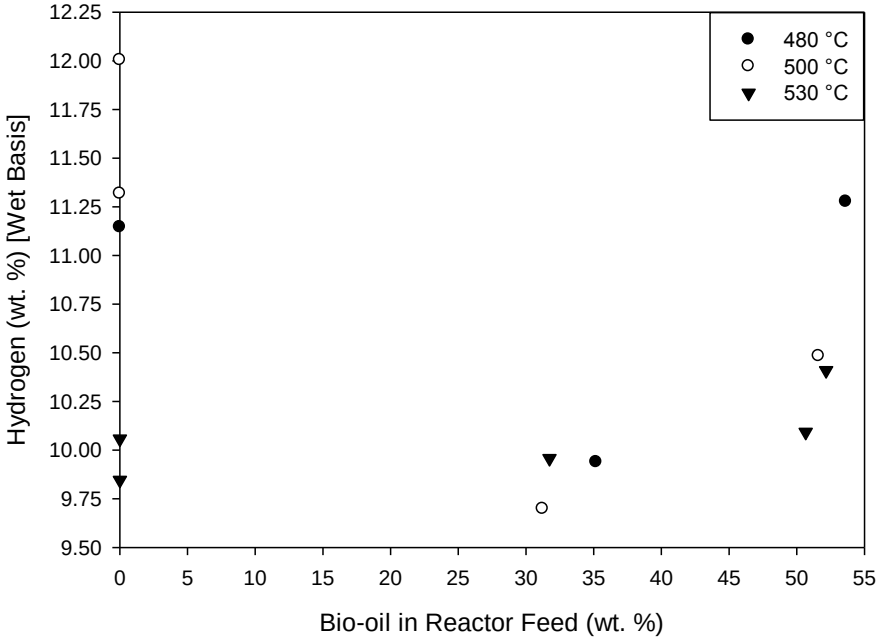

Figure A.2 Co-pyrolyzed ARC and Bio-oil Organic Phase Hydrogen Content

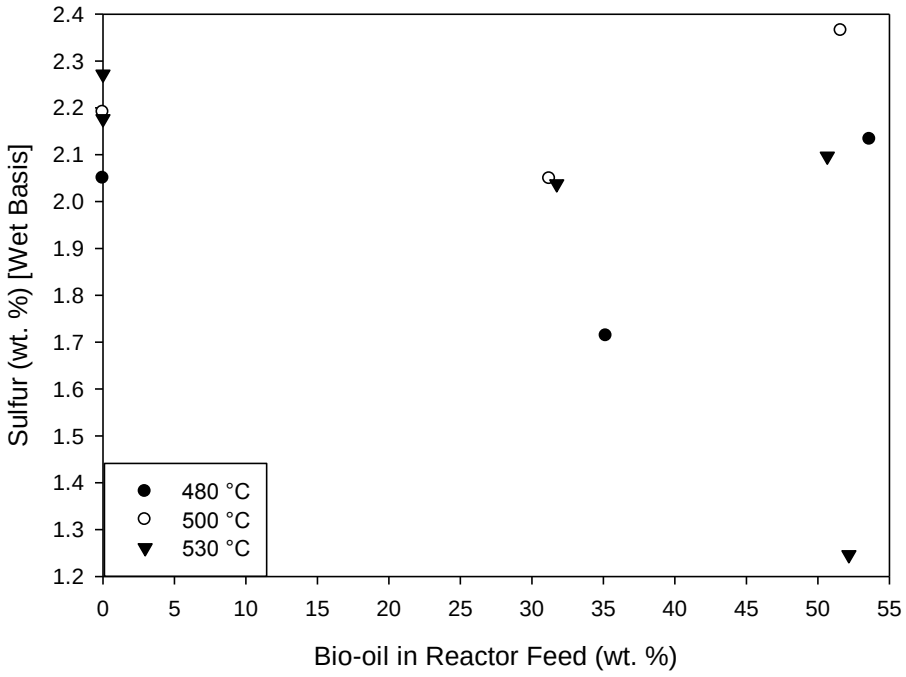

Figure A.3 Co-pyrolyzed ARC and Bio-oil Organic Phase Sulfur Content

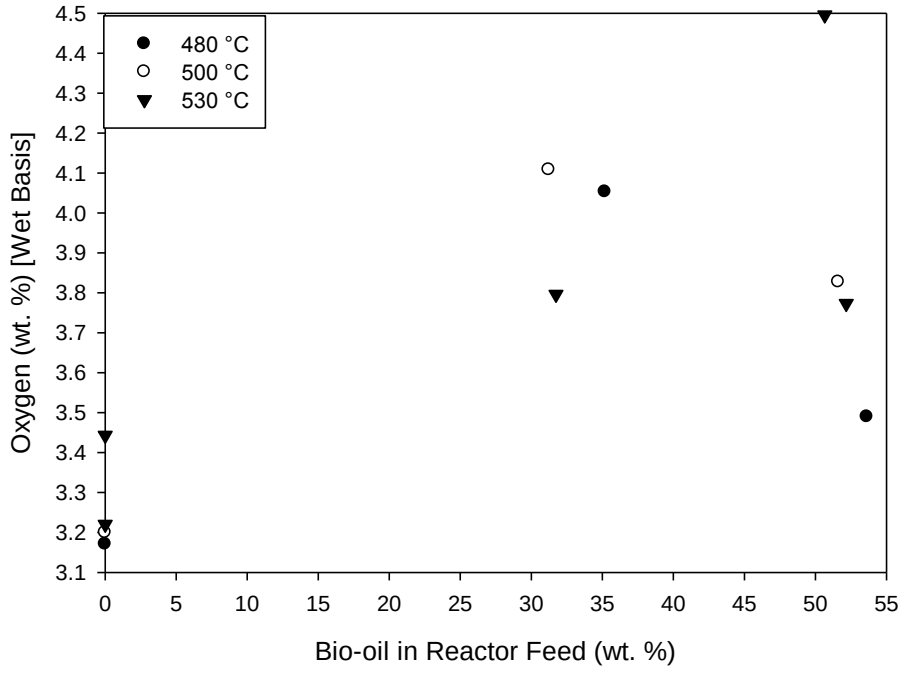

Figure A.4 Co-pyrolyzed ARC and Bio-oil Organic Phase Oxygen Content

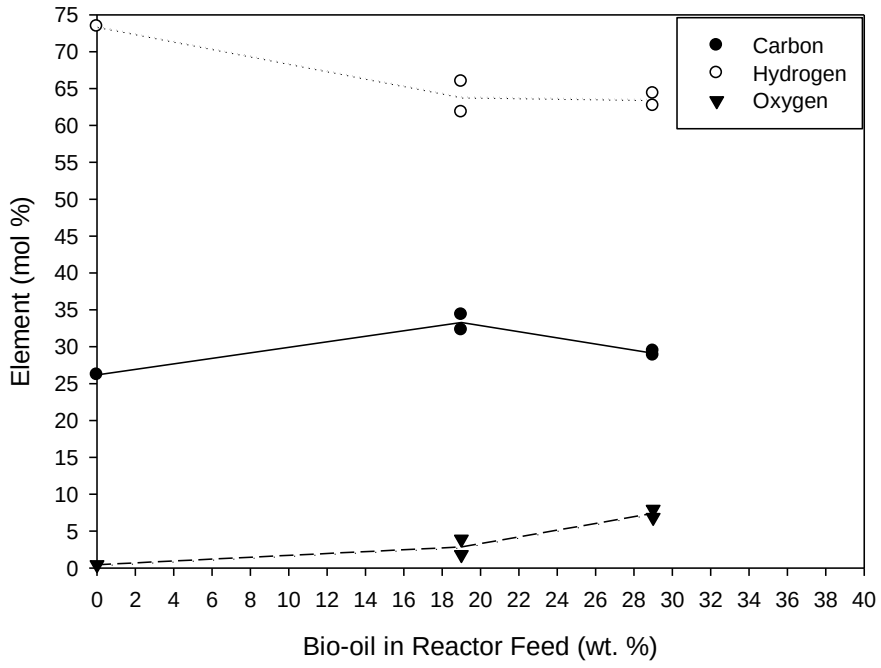

Figure A.5 Pyrolyzed Distillation Residue Gas Phase Atomic Composition at 480 °C

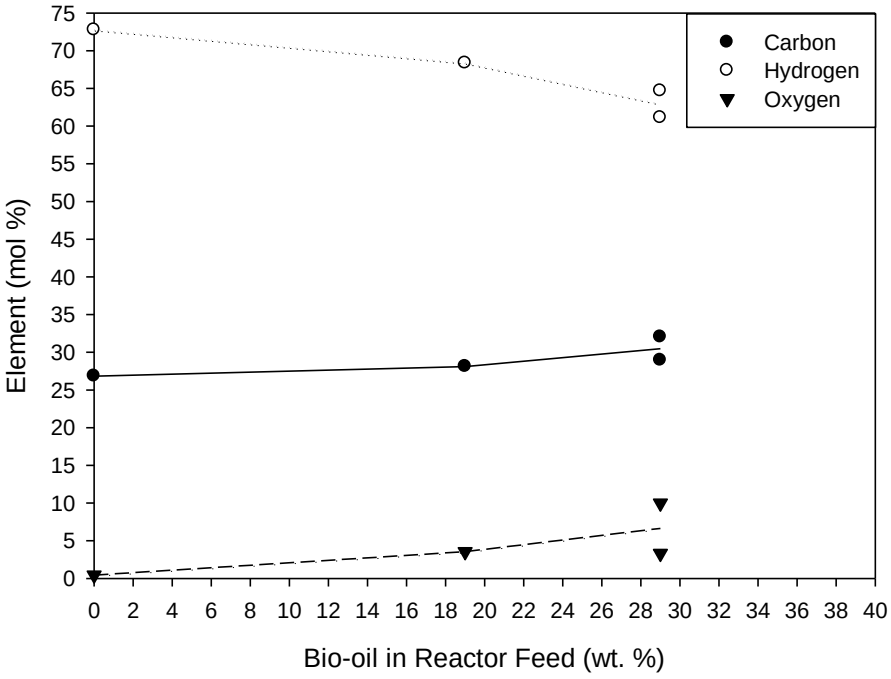

Figure A.6 Pyrolyzed Distillation Residue Gas Phase Atomic Composition at 500 °C

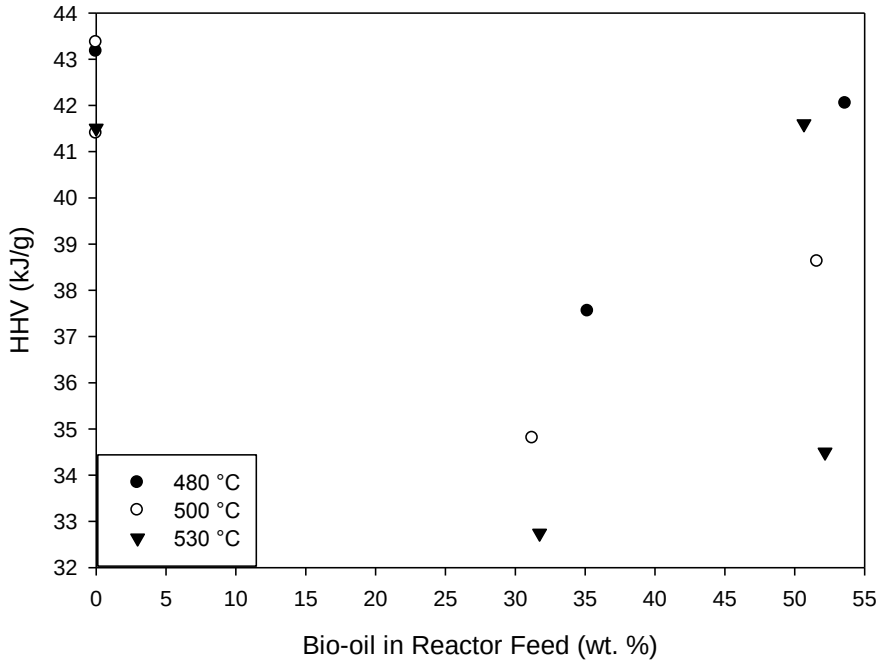

Figure A.7 Co-pyrolyzed ARC and Bio-oil Organic Phase High Heating Values

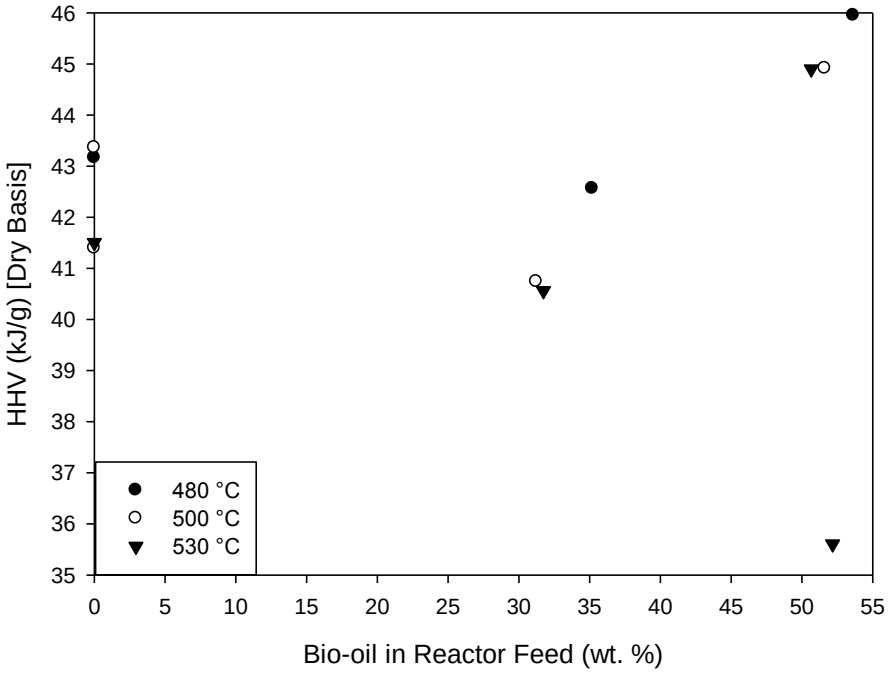

Figure A.8 Co-pyrolyzed ARC and Bio-oil Dry Basis Organic Phase HHVs

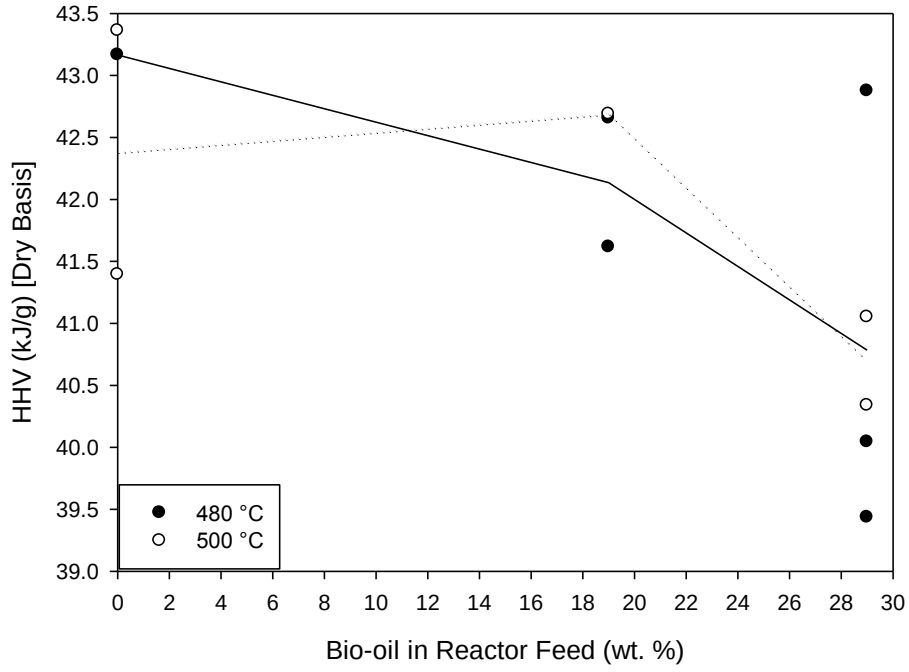

Figure A.9 Pyrolyzed Distillation Residue Dry Basis Liquid Product HHVs

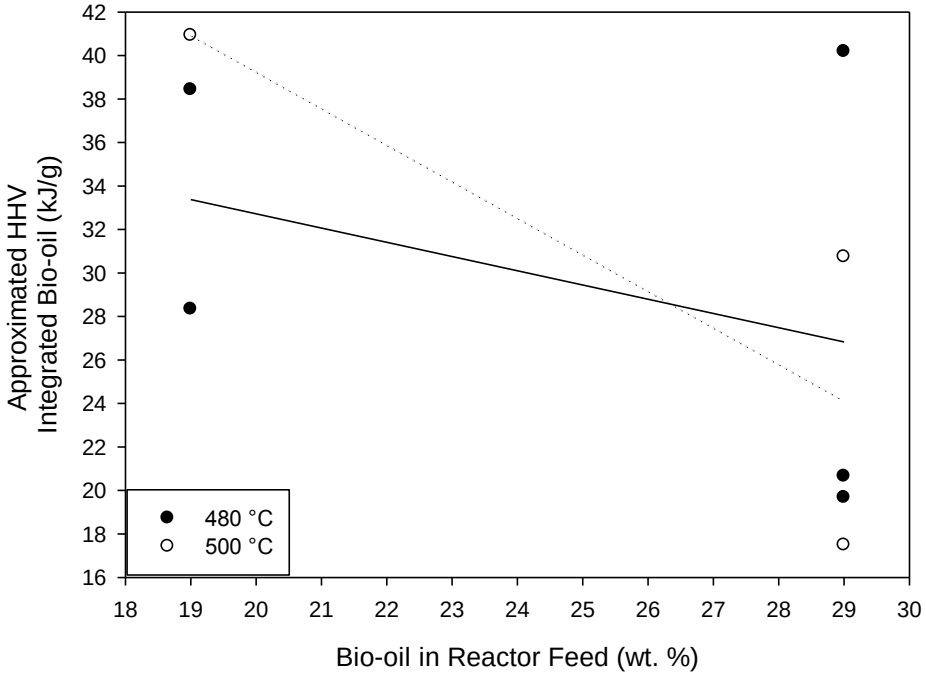

Figure A.10 Approximated Integrated Distillation Residue Bio-oil HHVs

Calculations were made to estimate the molecular composition of the refinery gas that would have been created if nitrogen gas was not used as a carrier gas, and the gas stream was processed to remove the 3-5 carbon hydrocarbons. The high heating values of the simulated refinery gases were calculated and the results are shown in figure A.11. The high heating values of the simulated refinery gas decreased with increasing proportions of bio-oil in the reactor feed.

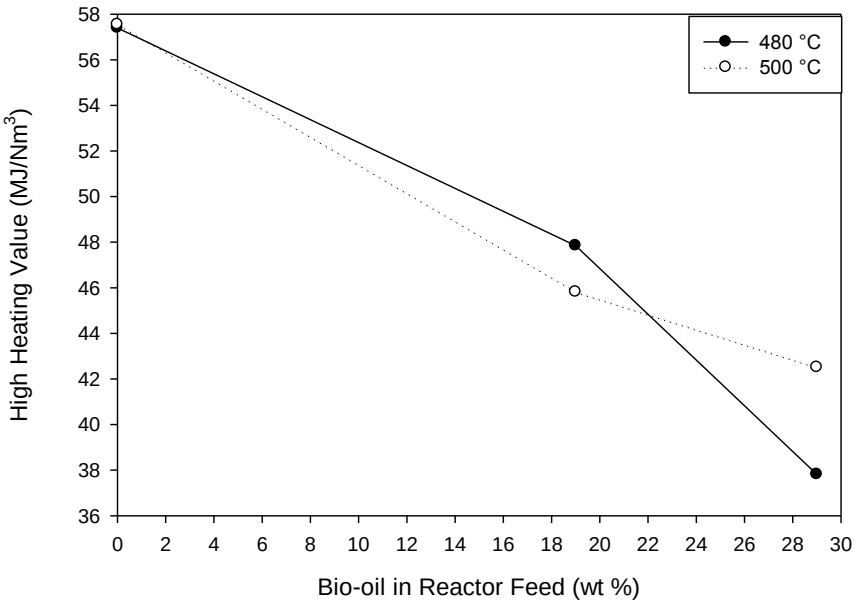

Figure A.11 Pyrolyzed Distillation Residue Refinery Gas High Heating Values

The gas yields for the co-pyrolysis of ARC and raw bio-oil are shown in figure A.12. As the gas yields were calculated by difference, the accuracy of the gas yields depended on the low accuracy of the solid yields. The gas yields from the pyrolysis of ARC increased when the reactor temperature was increased. The gas yields from the pyrolysis of raw bio-oil at 530 °C was 2.5 wt. % higher than the pyrolysis of raw bio-oil at 480-500 °C. There were no observable correlations for the gas yields when ARC was co-pyrolyzed with raw bio-oil.

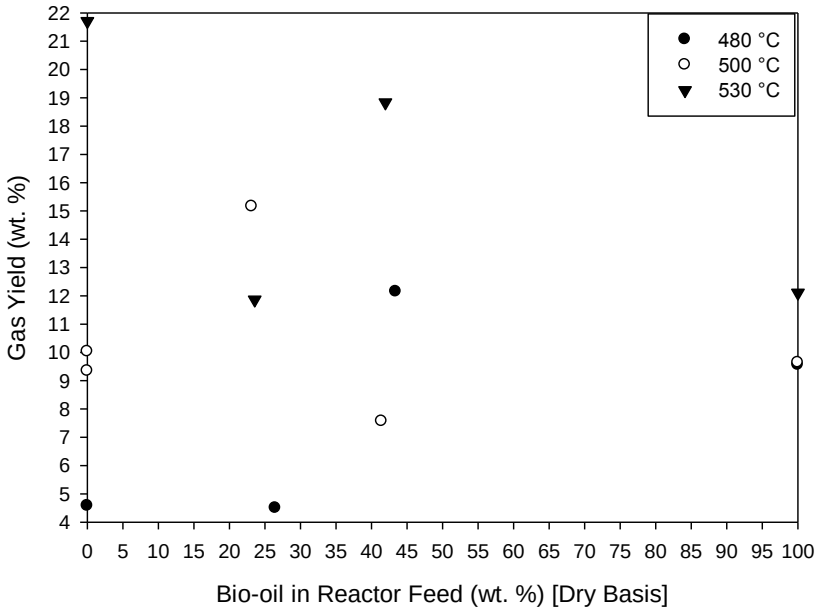

Figure A.12 Co-pyrolyzed ARC and Bio-oil Gas Yields

References

[1] (2013). 2013 Key World Energy STATISTICS, International Energy Agency, Paris, FR. [Online]. Available: http://www.iea.org/publications/freepublications/publication/KeyWorld2013_FINAL_WEB.pdf

[2] P. Frenzel, S. Fayyaz, R. Hillerbrand, A. Pfennig. "Biomass as Feedstock in the Chemical Industry - An Examination from an Exergetic Point of View." *Chem. Eng. Technol.*, vol 36, no. 2, pp. 233-240, 2013.

[3] (2011, 09). Paper #1-6 Unconventional Oil, The National Petroleum Council, Washington D.C., US. [Online]. Available: http://www.npc.org/Prudent_Development-Topic_Papers/1-6_Unconventional_Oil_Paper.pdf

[4] M. Brammer and Y. Reuter. (2009, 03). The Viability of Non-Conventional Oil Development, Innovest Strategic Value Advisors. London, UK. [Online]. Available: http://insideclimatenews.org/sites/default/files/Viability%20of%20Non-Conventional%20Oil.pdf

[5] (2013, 01). Issue Brief Biomass Carbon Neutrality, World Business Council for Sustainable Development, Conches-Geneva, CH. [Online]. Available: http://www.wbcsd.org/Pages/EDocument/EDocumentDetails.aspx?ID=15347

[6] T. Laan, T. A. Litman, R. Steenblik, "Biofuels – at What Cost? Government Support for Ethanol and Biodiesel in Canada," Global Subsidies Initiative, Geneva, CH, ISBN 978-1-894784-28-3, 2009.

[7] "Biofuels for a Better Climate How is the Tax Exemption Used?," The Swedish National Audit Office, Stockholm, SE, ISNM 978 91 7086 291 5, 2011.

[8] S. Hunt and R. Drigo, “A Review of the Current State of Bioenergy Development in G8 +5 Countries,” Global Bioenergy Partnership, Rome, IT, 2007.

[9] J.G. Speight, *Synthetic Fuels Handbook Properties, Process, and Performance*, 1st edition. New York, US: McGraw-Hill, 2008.

[10] D. Woolf, J.E. Amonette, F.A. Street-Perrott, J. Lehmann, and S. Joseph. “Sustainable Biochar to Mitigate Global Climate Change.” *Nat. Commun.* 1:56 doi: 1038/ncomms1053 (2010).

[11] D. Mohan, C.U. Pittman, P.H. Steele. “Pyrolysis of Wood/Biomass for Bio-oil: A Critical Review.” *Energ. Fuel*, vol 20, p. 848-889, 2006.

[12] J.E. Holladay, J.J. Bozell, J.F. White, and D. Johnson, “Top Value-Added Chemicals from Biomass Volume II—Results of Screening for Potential Candidates from Biorefinery Lignin,” Pacific Northwest Laboratory and the National Renewable Energy Laboratory, Richland, WA, US and Golden, CO, US, PNNL-16983, 2007.

[13] E. Sjostrom, *Wood Chemistry. Fundamentals and Applications*, 2nd edition. San Diego, CA, US: Academic Press, 1993.

[14] A. Bridgwater, “Thermal Biomass Conversion and Utilisation – Biomass Information System,” European Commission, Brussels, BE, EUR 16863, 1996.

[15] C. Peacocke and S. Joseph. (2009). Notes on Terminology and Technology in Thermal Conversion, International Biochar Initiative. Westerville, OH, US. [Online]. Available: http://www.biochar-international.org/images/Terminology.doc

[16] P. A. Brownsort, “Biomass Pyrolysis Processes: Performance Parameters and their Influence on Biochar System Benefits,” M.S. Dissertation, University of Edinburgh, Edinburgh, UK, 2009.

[17] J. A. Libra, K. S. Ro, C. Kammann, A. Funke, N. D. Berge, Y. Neubauer, M. Titirici, C. Fühner, O. Bens, J. Kern, and K. Emmerich. “Hydrothermal Carbonization of Biomass Residuals: a comparative Review of the Chemistry, Processes and Applications of Wet and Dry Pyrolysis” *Biofuels*, vol. 2, no 1, p. 89-124, Jan. 2011.

[18] R.Z. Vigouroux, “Pyrolysis of Biomass. Rapid Pyrolysis at High Temperatures. Slow Pyrolysis for Active Carbon Preparation,” PhD. Dissertation, Department of Chemical Engineering and Technology. Kungl Tekniska Högskolan, Stockholm, SE, 2001.

[19] T.B. Reed, J.P. Diebold, and R. Desrosiers, “Perspectives in Heat Transfer Requirements and Mechanisms for Fast Pyrolysis,” in *Specialists’ Workshop on Fast Pyrolysis of Biomass*, Copper Mountain, CO, US, 1980, p. 7-20.

[20] F.A. Agblevor, J.P. Diebold, and J. Scahill, “Alkali Metal Removal from Biocrude Oil: The Role of Char and Hot Gas Filtration Development.” National Renewable Energy Laboratory, Golden, CO, US, 1995.

[21] M. Nik-Azar, M. R. Hajaligol, M. Sohrabi, and B. Dabir. “Mineral Matter Effects in Rapid Pyrolysis of Beech Wood” *Fuel Process. Technol*, vol. 51, p. 7-17, 1997.

[22] A.V. Bridgwater, “Review of Fast Pyrolysis of Biomass and Product Upgrading.” *Biomass Bioenerg.*, vol 38, p. 68-94, 2012.

[23] M. Ringer, V. Putsche, and J. Scahill, “Large-Scale Pyrolysis Oil Production: A Technology Assessment and Economic Analysis,” National Renewable Energy Laboratory, Golden, CO, US, 2006.

[24] J.N. Brown, “Development of a Lab-scale Auger Reactor for Biomass Fast Pyrolysis and Process Optimization Using Response Surface Methodology,” M.S. Thesis, Department of Mechanical Engineering, Iowa State University, Ames, IA, US, 2009.

[25] R. Bayerbach, “Die Ablative Flashpyrolyse der PYTEC - Erste Erfahrungen und Produkteigenschaften,” PYTEC, Gülzow, DE, 2007.

[26] (2012, 08). Commercial Case Business Evaluation of Dynamotive’s Fast Pyrolysis and Upgrading Processes, Dynamotive Energy Systems. Vancouver, BC, CA [Online]. Available: http://www.dynamotive.com/assets/resources/2012/08/Dynamotive_Commercial_Case.pdf

[27] M. Garcia-Perez, T. Lewis, and C.E. Kruger “Methods for Producing Biochar and Advanced Biofuels in Washington State Part 1: Literature Review of Pyrolysis Reactors,” Washington State Department of Ecology, Spokane, WA, US, Ecology Publication Number 11-07-017, 2011.

[28] R.C. Brown, *Thermochemical Processing of Biomass Conversion into Fuels, Chemicals and Power*, 1st edition. West Sussex, UK: John Wiley & Sons, 2011.

[29] R.H. Venderbosch and W. Prins. “Fast Pyrolysis Technology Development.” *Biofuel. Bioprod. Bior.*, vol 4, p. 178-208, 2010.

[30] J.B. Jones, J.E. Holladay, C. Valkenburg, D.J. Stevens, C.W. Walton, C. Kinchin, D.C. Elliot , and S. Czernik, “Production of Gasoline and Diesel from Biomass via Fast Pyrolysis, Pacific Northwest National Laboratory, Richland, WA, US, PNNL-18284, 2009.

[31] B.M. Wagenaar, W. Prins, and W.P.M. Van Swaaij. “Pyrolysis of Biomass in the Rotating Cone Reactor: Modelling and Experimental Justification” *Chem. Eng. Sci.*, vol. 49, no 24B, p. 5109-5126, 1994.

[32] A.V. Bridgwater, “Fast Pyrolysis of Biomass for Energy and Fuels” in *Thermochemical Conversion of Biomass to Liquid Fuels and Chemicals*, M. Crocker, ed., 1st edition. Cambridge, UK: RSC, 2010 ch. 7, p. 146-191.

[33] A.V. Bridgwater, G.V.C. Peacocke. “Fast Pyrolysis Processes for Biomass.” *Renew. Sust. Energ. Rev.*, vol 4, p. 1-73, 2000.

[34] C. Roy. (2011, 05). Pyrovac Pyrolysis Oil and Biochar Production in Quebec, Pyrovac. Saint-Lambert, QC, CA. [Online]. Available: http://www.canbio.ca/events/quebec/presentations/roy_e.pdf

[35] C.E. Greenhalf, D.J. Nowakowski, A.B. Harms, J.O. Titiloye, and A.V. Bridgwater. “A Comparative Study of Straw, Perennial Grasses, and Hardwoods in Terms of Fast Pyrolysis Products.” *Fuel*, vol 108, p. 216-230, 2013.

[36] E. Jong, A. Higson, P. Walsh, and M. Wellisch, “Bio-based Chemicals Value Added Products from Biorefineries,” IEA Bioenergy Task 42 Biorefinery, 2012.

[37] P. de Wild, “Biomass Pyrolysis for Chemicals,” PhD dissertation, Department of Wiskunde en Natuurwetenschappen, Rijksuniversiteit Groningen, Groningen, NL, 2011.

[38] A. B. de Haan, G.W. Meindersma, J. Nijenstein, C. Vitasari, “A Techno-Economic Evaluation on the Feasibility of Chemicals from Pyrolysis Oil,” Eindhoven University of Technology, Eindhoven, NL, 2011.

[39] L. F. Žilnik and A. Jazbinšek. “Recovery of Renewable Phenolic Fraction from Pyrolysis Oil.” *Sep. Purif. Technol.*, vol. 86, p. 157-170, 2012.

[40] S. Czernik, A.V. Bridgwater. “Overview of Applications of Biomass Fast Pyrolysis Oil.” *Energ. Fuel.*, vol. 18, p. 590-598, 2004.

[41] W. V. Swaaij, G. V. Rossum, and S. Kersten. “Feeding Biomass into a Mineral Oil Refinery.” *Termotehnika*, vol 38, no. 2, p. 281-290, 2012.

[42] A. Oasmaa, C. Peacocke, “A Guide to Physical Property Characterisation of Biomass-derived Fast Pyrolysis Liquids,” VTT Technical Research Centre of Finland, FI, VTT Publications 450, 2001.

[43] A. Oasmaa, D.C. Elliott, and J. Korhonen. “Acidity of Biomass Fat Pyrolysis Bio-oils.” *Energ. Fuel.*, vol 24, p. 6548-6554, 2010.

[44] Y. Xu, Q. Liu, C. Zhang, W. Zhang, and Q. Zhang, “Increased Utilization of Bio-oil after Extraction and Separation of Carboxylic Acid.” In *2011 International Conference on Materials for Renewable Energy & Environment*, Shanghai, CN, 2011, p. 440-442.

[45] J. Lehto, A. Oasmaa, Y. Solantausta, M. Kytö, and D. Chiaramonti. “Fuel Oil Quality and Combustion of Fast Pyrolysis Bio-oils,” VTT Technical Research Centre of Finland, FI, VTT Technology 87, 2013.

[46] M. L. Honkela, T. R. Viljava, A. Gutierrez, and A. O. I. Krause, “Hydrotreating for Bio-oil Upgrading” in *Thermochemical Conversion of Biomass to Liquid Fuels and Chemicals*, M. Crocker, ed., 1st edition. Cambridge, UK: RSC, 2010 ch. 7, p. 146-191.

[47] J. G. Speight, *The Chemistry and Technology of Petroleum*, 5th edition. Boca Raton, FL, US: CRC Press, 2014.

[48] C. Branca, C. D. Blasi, and R. Elefante. “Devolatilization and Heterogeneous Combustion of Wood Fast Pyrolysis Oils.” *Ind. Eng. Res*, vol 44, p. 799-810, 2005.

[49] A. Oasmaa and S. Czernik. “Fuel Oil Quality of Biomass Pyrolysis Oils—State of the Art for the End Users.” *Energ. Fuel.*, vol 13, p. 914-921, 1999.

[50] E. Fratini, M. Bonini, A. Oasmaa, Y. Solantausta, J. Teixeira, and P. Baglioni. “SANS Analysis of the Microstructural Evolution During the Aging of Pyrolysis Oils from Biomass.” *Langmuir*, vol 22, p. 306-312, 2006.

[51] F.A. Agblevor, S. Bessler, and R.J. Evans, “Influence of Inorganic Compounds on Char Formation and Quality of Fast Pyrolysis Oils.” in *Abstracts of the ACS 209th National Meeting*, Anaheim, CA, US, 1995.

[52] Q. Zhang, J. Chang, T. Wang, Y. Xu. “Review of Biomass Pyrolysis Oil Properties and Upgrading Research.” *Energ. Convers. Manage.*, vol 48, p. 87-92, 2007.

[53] L. Deng, Y. Zhao, Y. Fu, Q. Guo. “Green Solvent for Flash Pyrolysis Oil Separation.” *Energy Fuels*, vol 23, p. 3337-3338, 2009.

[54] X. Zhang, G. Yang, H. Jiang, W. Liu, and H. Ding. “Mass Production of Chemicals from Biomass-derived Oil by Directly Atmospheric Distillation Coupled with Co-pyrolysis.” *Sci. Rep.* 3, 1120; DOI:10.1038/srep01120, 2013.

[55] J. Zheng and Q. Wei. “Improving the Quality of Fast Pyrolysis Bio-oil by Reduced Pressure Distillation.” *Biomass Bioenerg.*, vol 35, p. 1804-1810, 2011.

[56] E. Ceric, *Crude, Oil, Processes and Products.*, 1st edition. Sarajevo, BA: IBC d.o.o. , 2012.

[57] D.S.J. Jones, *Handbook of Petroleum Processing*, 1st edition. Dordrect, NL: Springer, 2006.

[58] G. L. Kaes, *Refinery Process Modeling A Practical Guide to Steady State Modeling of Petroleum Processes*, 1st edition. Colbert, GA, US: Kaes Enterprises, 2000.

[59] R. Sadeghbeigi, *Fluid Catalytic Cracking Handbook Design, Operation and Troubleshooting of FCC Facilities*, 2nd edition, Houston, TX, US: Gulf Publishing Company, 2000.

[60] A. A. Lappas, S. Bezergianni, and I. A. Vasalos. "Production of Biofuels via Co-processing in Conventional Refining Processes." *Catal. Today*, vol. 145, p. 55-62, 2009.

[61] G. Fogassy, Y. Schuurman, G. Toussaint, A. C. van Veen, and C. Mirodatos (2009, 11). Biomass Derived Feedstock Co-processing with VGO for Hybrid Fuel Production in FCC Units, Biocoup Project, [Online]. Available: http://www.biocoup.com/fileadmin/user/december/00_52_BIOCOUP_CNRS_Nov09.pdf

[62] F. M. Mercader, "Pyrolysis Oil Upgrading for Co-processing in Standard Refinery Units," PhD. Dissertation, Faculty of Science and Technology, University of Twente, Enschede, NL, 2010.

[63] F. A. Agblevor, O. Mante, R. McClung, and S. T. Oyama. "Co-processing of Standard Gas Oil and Biocrude Oil to Hydrocarbon Fuels." *Biomass Bioenerg*, vol. 45, p. 130-137, 2012.

[64] J. H. Gary and G. E. Handwerk, *Petroleum Refining Technology and Economics*, 4th edition. New York City, NY, US, 2001.

[65] Exxonmobil Research and Engineering Company, "Biomass Oil Conversion Process," US20110232164 A1, Mar, 1st, 2011.

[66] M. Chaudhari, “Effect of Liquid-Solid Contact on Thermal Cracking of Heavy Hydrocarbons in a Mechanically Fluidized Reactor,” M.E.S.c. Thesis, Department of Chemical and Biochemical Engineering, Western University, London, ON, CA, 2012.

[67] A. Oasmaa, E. Leppämäki, P. Koponen, J. Levander, and E. Tapola, “Physical Characterisation of Biomass-based Pyrolysis Liquids Application of Standard Fuel Oil Analyses,” VTT Technical Research Centre of Finland, FI, VTT Publications 306, 1997.

[68] M. Lackner, A. B. Palotás, and F. Winter, *Combustion From Basics to Application*. Weinheim, DE: Wiley-VCH Verlag GmbH & Co. KGaA, 2013.

[69] M. Kleinert, and T. Barth. “Towards a Lignincellulosic Biorefinery: Direct One-Step Conversion of Lignin to Hydrogen-Enriched Biofuel.” *Energ Fuel,* vol. 22, p. 1371-1379, 2008.

[70] M. A. Fahim, T. A. Al-Sahhaf, A. S. Elkilani, *Fundamentals of Petroleum Refining,* 1st ed. Kidlington, UK: Elsevier B. V., 2010.

[71] M. C. Samolada and I. A. Vasalos, “Catalytic Cracking of Biomass Flash Pyrolysis Liquids” in *Developments in Thermochemical Biomass Conversion Volume 1*, A. V. Bridgwater, ed., 1st edition. Bury St. Edmunds, UK: Chapman and Hall, 1997, p. 657-671.

[72] M. A. Sukiran, L. S. Kheang, N. A. Bakar, and C. Y. May. “Pyrolysis of Empty Fruit Branches: Influence of Temperature on the Yields and Composition of Gaseous Product.” *Am J Appl Sci,* vol 11, no. 4, p. 606-610, 2014.

[73] T. Dickerson and J. Soria. “Catalytic Fast Pyrolysis: A Review.” *Energies*, vol 6, p. 514-538, 2013.

[74] M. R. Rover, “Analysis of Sugars and Phenolic Compounds in Bio-oil,” Ph.D. dissertation, Biorenewable Resources and Technology, Iowa State University, Ames, IA, US, 2013.

[75] A. Jazbinšek, V. Grilc, L. F. Žilnik, “Isolation of Phenol and Phenolic Compounds from Fast Pyrolysis Bio-oil of Forestry Residue,” in *14th Slovenian Chemical Event*, Maribor, SI, 2008.

[76] G. Peacocke, P. Russel, J. Jenkins, A. Bridgewater. “Physical Properties of Flash Pyrolysis Liquids.” *Biomass Bioenerg*, vol 7, no 16, p. 169-177, 1994.

[77] N. M. Bennett, S. S. Helle, and S. J. B. Duff. “Extraction and Hydrolysis of Levoglucosan from Pyrolysis Oil.” *Bioresource Technol*, vol 100, no. 23, p. 6059-6063, 2009.

[78] J. K. S. Chan and S. J. S. B. Duff. “Methods for Mitigation of Bio-oil Extract Toxicity.” *Bioresource Technol*, vol 101, no. 10, p. 3755-3759, 2010.

[79] R. F. Probstein and R. E. Hicks, *Synthetic Fuels*, Dover edition. Mineola, NY, US: Dover Publications, 2006.

[80] S. Karatzos, J. D. McMillan, and J. N. Saddler, “The Potential and Challenges of Drop-in Biofuels,” IEA Bioenergy Task 39, T39-T1, 2014.

[81] R. Dabestani, P. F. Britt, and A. C. Buchanan. “Pyrolysis of Aromatic Carboxylic Acid Salts: Does Decarboxylation Play a Role in Cross-linking Reactions?.” *Prepr. Pap.-Am. Chem. Soc., Div. Fuel Chem.*, vol 48, no. 2, p. 565, 2010.

[82] B. Ettehadieh and S. Y. Lee, “Incineration of Low Quality MSW in the Rotary Water-cooled O’Connor Combustor,” in *1990 National Waste Processing Conference*, Long Beach, CA, US, 1990, p. 193-201.

[83] *GREET, The Greenhouse Gases, Regulated Emissions, and Energy Use in Transportation Model*, GREET 1.8d.1, 2010.

[84] R. B. Gupta and A. Demirbas, *Gasoline, Diesel and Ethanol Biofuels from Grasses and Plants*, 1st edition. New York, NY, US: Cambridge University Press, 2010.

Curriculum Vitae

Name: Ryan Lance

Post Secondary Education and Degrees:

The University of Western Ontario:

Masters Engineering Science in Chemical and Biochemical Engineering: 2015

The Ohio State University:

Bachelors of Science in Chemical Engineering: 2007